CONFIDENTIAL

Copy 333
RM L57C19

NACA RM L57C19

NACA

RESEARCH MEMORANDUM

INVESTIGATION AT MACH NUMBERS TO 1.04 OF BLADE-LOADING CHARACTERISTICS OF TWO FULL-SCALE THREE-BLADE SUPERSONIC PROPELLERS DIFFERING IN BLADE-SECTION CAMBER

By Leland B. Salters, Jr.

Langley Aeronautical Laboratory
Langley Field, Va.

Classification Changed to Unclassified
Authority: NASA Technical Publications
Announcement No. 8
Effective Date: July 22, 1959
WHL

CLASSIFIED DOCUMENT

This material contains information affecting the National Defense of the United States within the meaning of the espionage laws, Title 18, U.S.C., Secs. 793 and 794, the transmission or revelation of which in any manner to an unauthorized person is prohibited by law.

NATIONAL ADVISORY COMMITTEE
FOR AERONAUTICS

WASHINGTON

September 12, 1957

CONFIDENTIAL

NATIONAL ADVISORY COMMITTEE FOR AERONAUTICS

RESEARCH MEMORANDUM

INVESTIGATION AT MACH NUMBERS TO 1.04 OF BLADE-LOADING CHARACTERISTICS OF TWO FULL-SCALE THREE-BLADE SUPERSONIC PROPELLERS DIFFERING IN BLADE-SECTION CAMBER

By Leland B. Salters, Jr.

SUMMARY

Total-pressure surveys were made in the slipstreams of two full-scale three-blade supersonic propellers in the Langley 16-foot transonic tunnel at Mach numbers up to 1.04 to determine the effects of camber on supersonic-propeller characteristics. The two propellers were similar except that one of them had symmetrical blade sections and the other had cambered blade sections and a slightly different pitch distribution. Integrated thrust coefficients were in good agreement with the force data. Because of limitations in dynamometer rotational speed the investigation did not extend to the design speed of the propellers.

Over the complete range of the tests the cambered propeller maintained the higher thrust and efficiency. The reactions of the propeller blade sections to compressibility, such as a lift increase with increase in Mach number and the force break, were qualitatively similar to those of two-dimensional airfoil data.

INTRODUCTION

In the initial stages of supersonic-propeller development, the propeller design was based on calculations using two-dimensional airfoil data. These calculations showed that a reduction in blade camber as well as blade-section thickness resulted in an increase in propeller efficiency, the optimum efficiency being obtained with zero camber and zero thickness. A supersonic propeller designed during this period was investigated and reported in references 1 and 2. It was a three-blade, 9.75-foot-diameter propeller of Curtiss-Wright design number 109622 embodying thin airfoil sections (6 percent at spinner, 2 percent at tip) of zero camber.

Propellers using such thin airfoil sections characteristically suffer from flutter sensitivity, especially when operating at conditions of take-off and climb. Certain propeller tests such as those reported in reference 3 indicated that the introduction of camber into propeller blade design would improve flutter characteristics. However, the effects of camber on the aerodynamic characteristics of propellers operating in the transonic regime was unknown.

Another propeller of Curtiss-Wright design number 109626 was therefore designed identical to the 109622 except that camber was incorporated in the blades and except for a slight change in pitch distribution. The opportunity presented itself for investigating the effects of camber on the aerodynamic characteristics of a supersonic propeller by testing the Curtiss-Wright 109626 propeller and comparing results with those of the Curtiss-Wright 109622 propeller.

With this in view the present investigation was initiated in which the Curtiss-Wright 109626 propeller was tested at comparable operating conditions to that of the original investigation of the Curtiss-Wright 109622 propeller. Because of improvement in test equipment of the present investigation the Mach number range was extended from 0.96 up to 1.04. Wake survey data were obtained as in the previous investigation for determining the blade-loading characteristics, checking the force data (ref. 4), and in general adding to the thoroughness of the investigation.

The purpose of this paper is to present the wake-survey data of the Curtiss-Wright 109626 propeller and some comparisons with the Curtiss-Wright 109622 propeller which may aid in isolating and identifying the effects of camber on the aerodynamic characteristics of a supersonic propeller. This investigation covered a range of blade angles at the 0.75 radial station of 46.8° to 64.4° in approximately 5° increments and a Mach number range from 0.60 to 1.04.

SYMBOLS

B	number of blades
b	blade chord, ft
C_T	thrust coefficient, $\frac{T}{\rho n^2 D^4}$
c_l	section lift coefficient
c_{l_d}	section design lift coefficient

c_t	section thrust coefficient
D	propeller diameter, ft
h	blade-section thickness, ft
J	advance ratio, $\frac{V}{nD}$
M	tunnel airstream Mach number
M_x	helical section Mach number, $M\sqrt{1 + \left(\frac{\pi x}{J}\right)^2}$
n	propeller rotational speed, rps
$\{\Delta p_t\}$	time average of stagnation-pressure rise through the propeller
R	propeller-tip radius, ft
r	radius to blade element, ft
T	thrust, lb
V	tunnel airstream velocity, ft/sec
x	fractional radius to propeller blade section, r/R
α_a	absolute angle of attack (measured from zero lift line), deg
$\Delta\alpha_a$	difference in absolute angle of attack between 109622 and 109626 blades, $(\alpha_a)_{109626} - (\alpha_a)_{109622}$, deg
β	propeller blade angle, deg
$\beta_{0.75R}$	blade-angle setting at 0.75 radial station, deg
$\Delta\beta$	difference in blade angle between 109622 and 109626 blades, $\beta_{109626} - \beta_{109622}$, deg
ρ	mass density of air, slugs/cu ft
ρ_t	stagnation density, slugs/cu ft

APPARATUS

Propeller Dynamometer

The 6,000-horsepower propeller dynamometer as described in reference 5 and shown in figures 1 and 2 was mounted in the test section of the Langley 16-foot transonic tunnel. The test configuration was similar to that of the original tests (refs. 1 and 2) except for minor modifications. The principal changes (see ref. 4) consisted of the relocation of the propeller 3 feet forward of the former axial location and the addition of a fairing between the two dynamometer support struts. These modifications permitted an increase in free-stream test Mach number from 0.96 to 1.04.

Propellers

The three-blade, 9.75-foot-diameter propeller designated as the Curtiss-Wright design number 109626 is shown in figure 1 and described in reference 4. Blade-form curves are given in figure 3. The blades were of solid steel and designed for a four-blade, 10-foot-diameter propeller configuration with peak efficiency at 35,000-foot altitude, 2,600 rpm, a Mach number of 0.95, and an advance ratio of 2.2.

The Curtiss-Wright 109622 propeller as described in reference 1 was also used in this investigation, being similar to the Curtiss-Wright 109626 except for blade-section camber and a slight difference in pitch distribution as described in reference 4. Hereafter in this paper the two propellers will be designated by their design numbers only.

Wake-Survey Rakes

The two rakes used in this investigation incorporated static- and total-pressure tubes with radial positions from $x = 0.324$ to 1.406. Figure 4 gives the details of the rakes and figure 1 shows the rakes installed in the tunnel test section.

As explained in reference 2 the ideal angular location of the rakes is 180° apart; the reason for the location shown (45° apart) was to lessen the 1-P vibratory stresses in the propeller blades produced by a slight angularity in the airstream.

The rake orifices were located 51 inches (0.44 propeller diameters) behind the propeller plane of rotation.

TESTS

During most of the tests the tunnel Mach number was held at a constant value while the rotational speed was varied from that of approximately zero power input up to that of the upper power limit of the dynamometer except where the rotational speed was limited to lower values because of propeller flutter. The blade angle at the 0.75 radial station was varied from 46.8° to 65.4° in approximately 5° increments and the free-stream Mach number from 0.60 to 1.04. The test Mach numbers and the average nominal blade angles where possible were made identical with those of the original investigation of references 1 and 2 so that comparisons could be made between the cambered and uncambered propellers at the same advance ratios. It may be noted that this gives greatly different power absorptions for the two propellers because of the differences in absolute angle of attack of the blade sections. Data were also obtained for comparisons at conditions of peak efficiency.

Several tests were made at a constant Mach number of 0.13 with blade angles at the 0.75 radial station varying from 16.4° to -13.0° in approximately 5° increments.

In order to extend the Mach number range covered in the previous investigation of the 109622 uncambered propeller as reported in references 1 and 2, several tests were made with this propeller at the higher Mach numbers from 0.96 to 1.04.

REDUCTION OF DATA

The method used for computing the section thrust and section lift coefficients from rake data is presented in reference 6, wherein the following equations for the blade-section thrust and lift coefficients are derived:

$$c_t = \frac{1}{4} \frac{J^2 \pi x \left\{\Delta p_t\right\}}{\frac{1}{2}\rho_t V^2}$$

$$c_l = \frac{\left\{\Delta p_t\right\}}{\frac{1}{2}\rho_t V^2} \frac{J}{B\frac{b}{D}\sqrt{1 + \left(\frac{\pi x}{J}\right)^2}}$$

where $\left\{\Delta p_t\right\}$ is obtained directly from total-pressure measurements.

As in reference 2, the curves of section thrust and section lift coefficients represent the averages of the curves for each rake. The effect of rotation of the slipstream was neglected in these results because calculations showed that in the most extreme cases this correction would be less than 1 percent.

RESULTS AND DISCUSSION

Integrated Thrust Coefficients of Curtiss-Wright 109626 Propeller

In figures 5 and 6 is shown a comparison of the results of the wake-survey data with those of the force data. The force-data points are indicated by circles and wake survey by squares. The lines represent faired force-data curves as presented in reference 4.

Although some minor changes had been made to the test apparatus since the investigation of the 109622 propeller as presented in references 1 and 2, the results of the present investigation are similar to those of the former. As discussed in reference 2, the probable reason for most of the discrepancy that exists between the wake survey and force data is that the rakes were not ideally located with respect to the slipstream.

Originally the rakes had been located 135° apart and under these conditions the wake survey data had been in excellent agreement with the force data (ref. 2). With the rakes in the original position, however, there existed an angularity in the tunnel air flow of such magnitude that propeller tests were limited to free-stream Mach numbers of 0.60 and below. (This limitation was due to excessive stresses in the propeller blades due to 1-P vibrations produced by angularity in the airstream.) The rakes were therefore relocated in such a way that the flow angularity was reduced. In the final position of the rakes (45° apart) as used in the present investigation, the propellers could be tested to a Mach number of 1.04, and the agreement between wake-survey and force data was satisfactory, although not as good as when the rakes were 135° apart, as discussed in reference 2.

It may be noted that over the whole Mach number range, almost without exception, the agreement was better for the lower blade angles than for the higher blade angles. The differences between the force and wake-survey data showed no consistent variation with Mach number for either propeller.

Thrust Loading at Constant Advance Ratios

Figure 7 shows the thrust loading distributions along the 109626 propeller blade for advance ratios from 2.24 to 4.30, for Mach numbers from 0.60 to 1.04, and for blade angles at the 0.75 radial station from 46.8° to 64.4°. The Mach number range was limited to 0.60 and 0.70 for blade angles of 46.8° and 52.2° by the maximum propeller rotational speed. At the lower values of advance ratio the thrust peaks occurred in general near the blade station $x = 0.90$. The peaks appear to shift inboard slightly with increase in advance ratio until at $J = 4.30$ the peaks are near $x = 0.80$ to 0.85. The reason for this shift is the relative increase in loading of the inboard sections as compared with outboard sections as advance ratio is increased, as explained in reference 7, figure 29.

Figure 8 is a cross plot of the data of figure 7 to illustrate the effect of Mach number on the thrust loading of the propeller blade at a representative station ($x = 0.70$) for several values of advance ratio. As the Mach number increases from 0.60 to 0.80 or 0.85 the section thrust increases, then from there up to a Mach number of 1.00 there is a sharp decrease in section c_t followed by a rise beyond Mach number 1.00. These curves follow the familiar pattern of airfoil lift plotted against Mach number at constant angle of attack which indicates that compressibility phenomena for a propeller blade section is similar in general to that associated with two-dimensional airfoil characteristics.

Thrust Loading at Advance Ratios for Maximum Efficiency

The thrust loading variation with Mach number at a high blade angle and at advance ratios for maximum efficiency is shown in figure 9 for the 109626 propeller. The data were from the same tests as for figure 7(d) for purposes of comparison.

Comparing figure 7(d) with figure 9, it may be observed that the large spread in integrated thrust coefficients (fig. 7(d)) with variation in Mach number was due to the fact that the higher Mach number curves were for an advance ratio greater than that for maximum efficiency and the lower Mach number curves were for an advance ratio less than that for maximum efficiency. The spread is not nearly so great when the propeller is operating at advance ratios for maximum efficiency (fig. 9).

Referring to figure 9, it may be seen that as the Mach number is increased from 0.60 to 0.80 the section thrust coefficient increases over the whole blade but that the increase is greater for the outboard than for the inboard sections. From Mach number 0.80 to 0.89 the outboard sections remain practically the same but the inboard sections show a decrease in thrust. Then at Mach numbers 1.00 and 1.03 there is an

overall drop in thrust, the larger decrease occurring for the inboard sections. This indicates that compressibility effects are greater for the inboard sections than for the outboard sections. This effect is due to the greater thickness ratio and greater camber of the inboard sections relative to the outboard sections. Figure 10 of reference 2 shows this effect is less pronounced for the propeller with symmetrical blade sections.

Lift Distribution at Advance Ratios for Maximum Efficiency

Figure 10 shows the section lift-coefficient distribution on the propeller blade from spinner to tip at advance ratios for maximum efficiency for a blade angle at the 0.75 radial station of 61.6° and for Mach numbers from 0.60 to 1.03. The data presented in this figure are for the same runs and points as for figure 9 to illustrate the relationship between section thrust and lift coefficients.

At a Mach number of 0.60 the variation of section lift coefficient is almost linear from spinner to tip, the inboard sections having the higher values. For Mach number 0.80 the pattern is almost the same but the values are greater in magnitude. At a Mach number of 0.89 compressibility losses make their appearance as in figure 8. At Mach numbers of 1.00 and 1.03 compressibility losses are very apparent, as in figure 8. The particular contribution of figure 10 is the insight given into the effect of compressibility upon the section lift distribution. It may be seen that the lift is decreased more in the central portions of the blade than for the inboard or outboard sections, forming a saddle.

Thrust Distributions for Negative Blade Angles

Figure 11 was included in this paper to give an indication of the thrust distribution over the propeller blade while the propeller is being used as a brake. The 109626 propeller was operating at 650 rpm, a blade angle of -13.6° at the 0.75 radial station, and a Mach number of 0.13. The large magnitude of the negative thrust coefficient indicates the effectiveness of the propeller when used as a brake.

It may be observed that the slipstream, as registered on the rake, is 25 percent larger in diameter than the propeller. This would indicate that the slipstream has expanded 25 percent in the 0.44 propeller-diameter distance between propeller and rake.

Thrust Loading Comparisons Between the Cambered and Uncambered Propellers at Constant Advance Ratio

In figure 12 are presented some direct comparisons between the section thrust loading distributions of the 109622 (uncambered) and the 109626 (cambered) propellers at the constant advance ratio of 3.90. Data for the uncambered propeller (figs. 12(a) and 12(b)) are from reference 2.

The differences in fairing between the curves of reference 2 and this investigation near the spinner and near the tips require some explanation. In the investigation of reference 2 the total-pressure probes were located 4 inches apart but in the present investigation were located 1.33 inches apart. Also there were two probes nearer the spinner in the present investigation. In the former the curves were faired to the spinner because the inmost probes were outside the boundary layer and gave no indication of the extent or character of the boundary layer. The additional probes, in the present investigation, extended into the boundary layer and furnished the information required to define the curve more accurately. Also in the investigation of reference 2 the rake was located 17 inches behind the propeller plane of rotation, whereas in the present investigation the rake was located 51 inches behind the propeller. For the present investigation the slipstream had more time and distance after leaving the propeller in which to alter its shape and distribution before reaching the probes. This and the closer spacing of probes in the present investigation, which gave better definition, explain why the boundary of the slipstream, as registered at the rake, did not always coincide with the propeller-tip radial station.

Another factor should be pointed out in comparing the thrust loading curves shown in figure 12. Due consideration must be given to the difference in pitch distribution and blade-angle setting when making direct comparisons of the thrust loading curves of the 109622 and 109626 propellers. In figure 13 is shown the section pitch distribution along the blades of the 109626 (cambered) and the 109622 (uncambered) propellers with the blade angles at the 0.75 radial station set 1.4° apart, the cambered blade having the greater pitch. The 1.4° pitch differential was chosen as typical of those used in the two investigations, although 1.6° differential was often used. From this it may be seen that the cambered propeller had the greater pitch near the tip and less at the inboard sections than the uncambered propeller (see $\Delta\beta$, fig. 13). The section absolute angle-of-attack differential between the cambered and uncambered blades is shown as $\Delta\alpha_a$ in figure 13. This shows the cambered propeller to have the greater section absolute angle of attack (from about 1.0° at $x = 0.425$ to about 3.2° at $x = 0.85$). The fact that the absolute angle-of-attack differential was greater at the tip than inboard probably explains why the peak section-thrust-coefficient

values in figure 12 occur nearer the tip for the cambered than for the uncambered propeller. Also the larger integrated thrust coefficients of the cambered propeller when compared to the uncambered propeller at equal advance ratios may be explained by the fact that the section absolute angles of attack for the cambered propeller are greater over the entire blade.

Thrust Loading Comparisons Between the Cambered and Uncambered Propellers at Advance Ratios for Maximum Efficiencies

Thrust loadings of the 109626 (cambered) propeller at advance ratios for maximum efficiency are compared in figure 14 with those for the 109622 (uncambered) propeller. Data were obtained from the same tests as used in figure 12, except that test points were chosen for maximum efficiency rather than for constant advance ratio. The propellers could not be compared at conditions for which they were designed (advance ratio of 2.2 and about 45° blade angle) because of limitations in rotational speed and therefore the comparisons shown are for off-design conditions for both propellers. At these off-design conditions shown in figure 14 the efficiency of the cambered propeller is the higher in every case which would indicate that at this Mach number and thrust-coefficient range the cambered propeller blade sections had the higher values of lift-drag ratio. Calculations in reference 4 for other thrust coefficients and Mach numbers indicate that near the design conditions the uncambered propeller has about 3 percent greater efficiency than the cambered propeller.

Figure 14 indicates clearly the characteristic differences in the way the thrust coefficients for maximum efficiency of the cambered and uncambered propellers vary with Mach number. The magnitude of the thrust coefficients for maximum efficiency of the uncambered propeller decreases slightly from a Mach number of 0.60 to 0.80 and then rises steadily from a Mach number of 0.80 up to 1.03. In contrast, those for the cambered propeller increase rapidly from a Mach number of 0.60 to a peak between 0.80 and 0.89 and then decrease sharply down to 1.00, with little change from there to 1.03. At a Mach number of 0.80, as shown in figure 14(b), the magnitude of the thrust coefficient for maximum efficiency for the cambered propeller is about twice that for the uncambered propeller, but at Mach numbers 1.00 and 1.03 (figs. 14(d) and 14(e)) the difference is much less. This would indicate that the effects of compressibility are greater for the cambered than for the uncambered propeller.

CONCLUSIONS

A wake-survey investigation of the thrust loadings on the blades of two full-scale three-blade supersonic propellers was made at Mach numbers up to 1.04 to determine the effect of camber on supersonic propeller characteristics. Although the propellers could not be tested at their design conditions due to limitations in rotational speeds, over the whole range of off-design conditions of this investigation, the cambered propeller maintained the higher efficiency and the greater thrust. This effect was more pronounced at the subsonic Mach numbers. Thrust coefficients obtained from integrated wake-survey data were in good agreement with those obtained from force data, particularly at the lower blade angles.

A study of the thrust loading distributions led to the following conclusions:

1. The effects of compressibility upon the blade-section elements in the propeller are similar to the effects upon two-dimensional airfoil characteristics.

2. Losses in thrust due to compressibility effects are greater for the cambered propeller than for the propeller with symmetrical blade sections.

3. Losses in thrust due to compressibility for the cambered propeller are greater for the thick inboard than for the thin outboard blade sections. This effect was less pronounced for the propeller with symmetrical blade sections.

Langley Aeronautical Laboratory,
National Advisory Committee for Aeronautics,
Langley Field, Va., March 6, 1957.

REFERENCES

1. Evans, Albert J., and Liner, George: A Wind-Tunnel Investigation of the Aerodynamic Characteristics of a Full-Scale Supersonic-Type Three-Blade Propeller at Mach Numbers to 0.96. NACA RM L53F01, 1953.

2. Swihart, John M., and Norton, Harry T., Jr.: Wake Surveys in the Slipstream of a Full-Scale Supersonic-Type Three-Blade Propeller at Mach Numbers to 0.96. NACA RM L53I09, 1953.

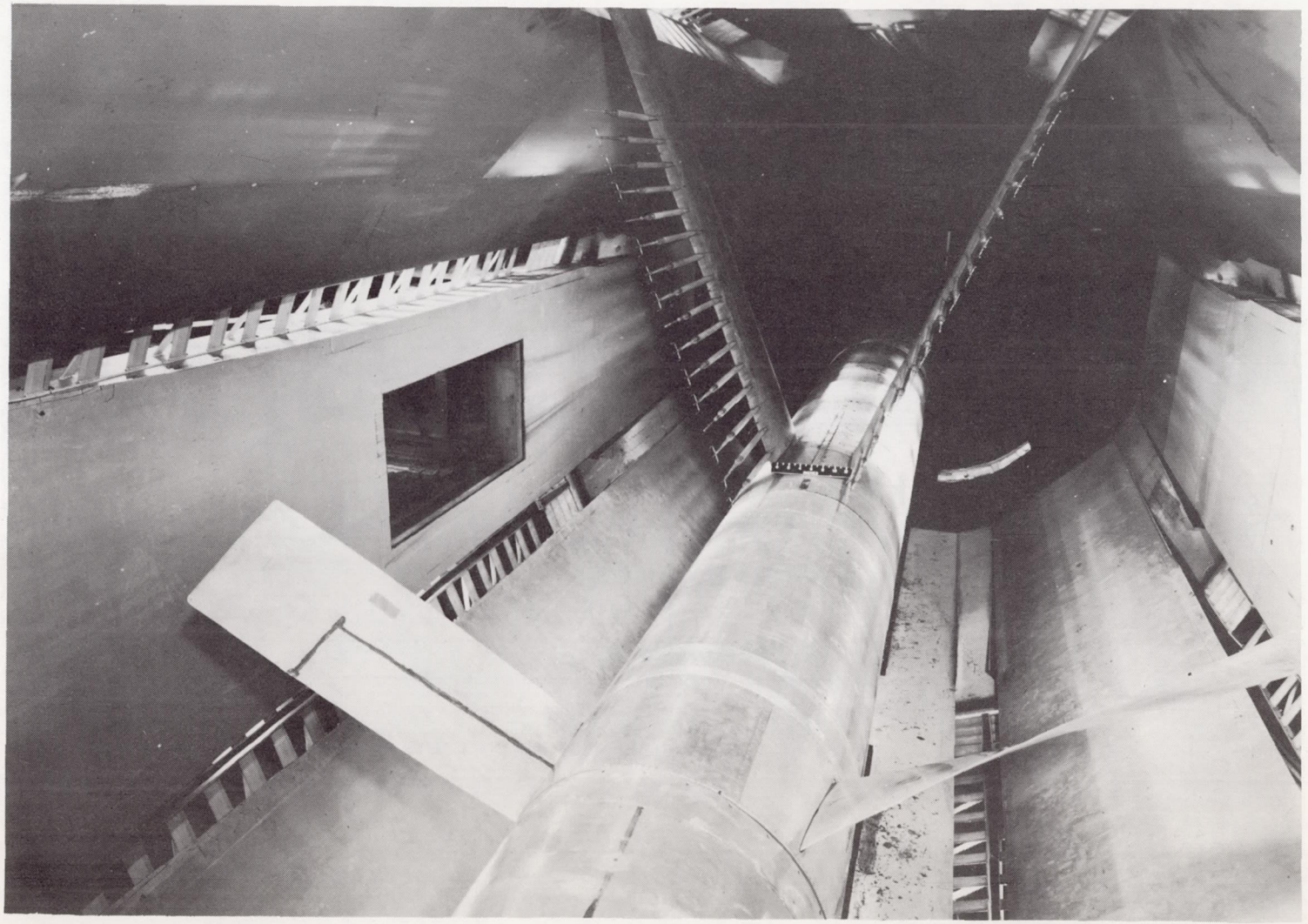
3. Allis, Arthur E., and Swihart, John M.: The Effect of Blade-Section Camber on the Stall-Flutter Characteristics of Three NACA Propellers at Zero Advance. NACA RM L53B17, 1953.

4. Maynard, Julian D., Swihart, John M., and Norton, Harry T., Jr.: Effect of Blade-Section Camber on Aerodynamic Characteristics of Full-Scale Supersonic-Type Propellers at Mach Numbers to 1.04. NACA RM L56E10, 1956.

5. Wood, John H., and Swihart, John M.: The Effect of Blade-Section Camber on the Static Characteristics of Three NACA Propellers. NACA RM L51L28, 1952.

6. Davidson, Robert E.: Propeller Lift and Thrust Distribution From Wake Surveys of Stagnation Conditions. NACA RM L51K29, 1952.

7. Gilman, Jean, Jr.: Wind-Tunnel Tests and Analysis of Three 10-Foot-Diameter Three-Blade Tractor Propellers Differing in Pitch Distribution. NACA WR L-712, 1946. (Formerly NACA ARR L6E22.)



L-86111

Figure 1.- The 6,000-horsepower propeller dynamometer mounted in the Langley 16-foot transonic tunnel with propeller and wake survey rakes installed.

CONFIDENTIAL

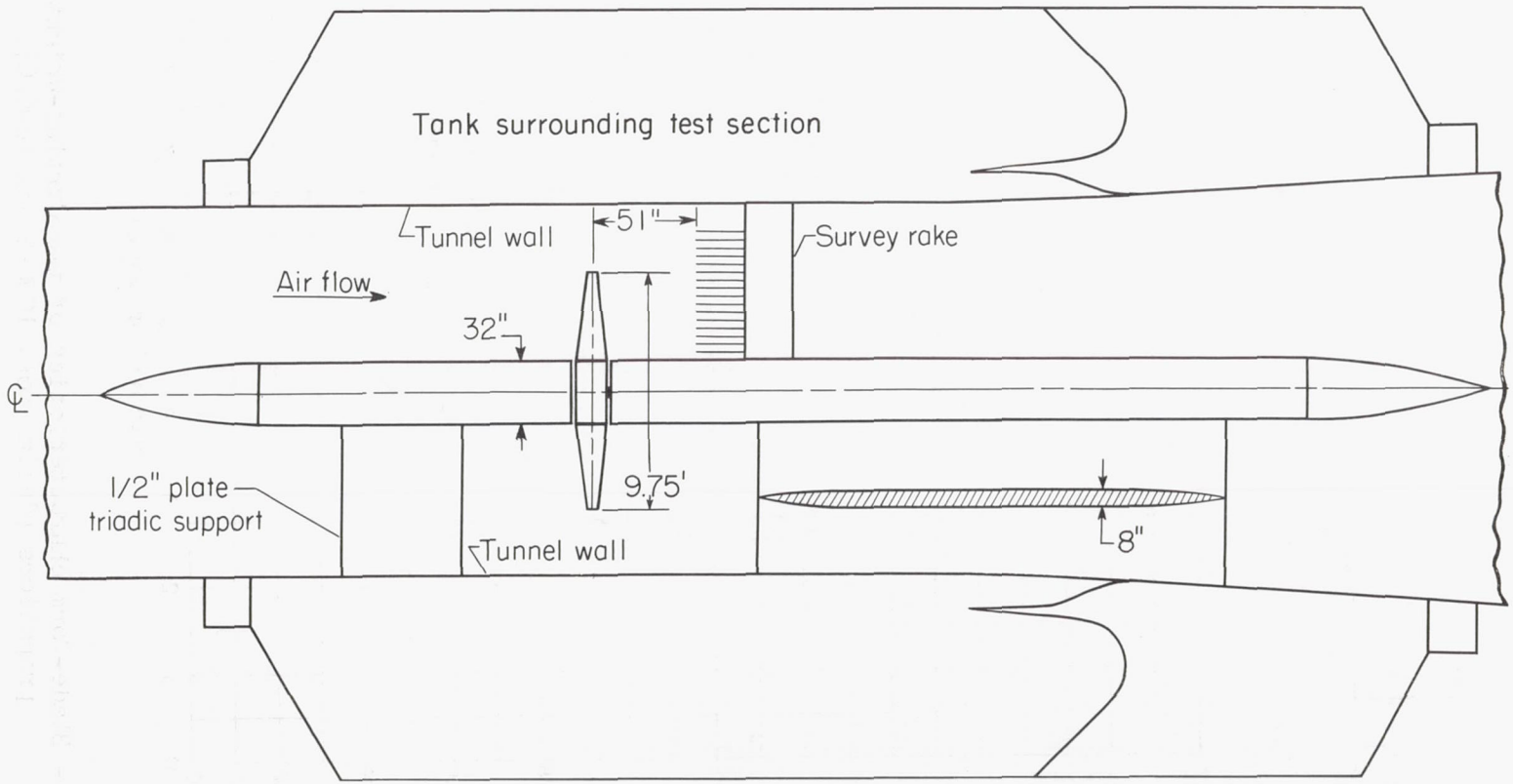


Figure 2.- Dynamometer and survey-rake installation in the test section of the Langley 16-foot transonic tunnel.

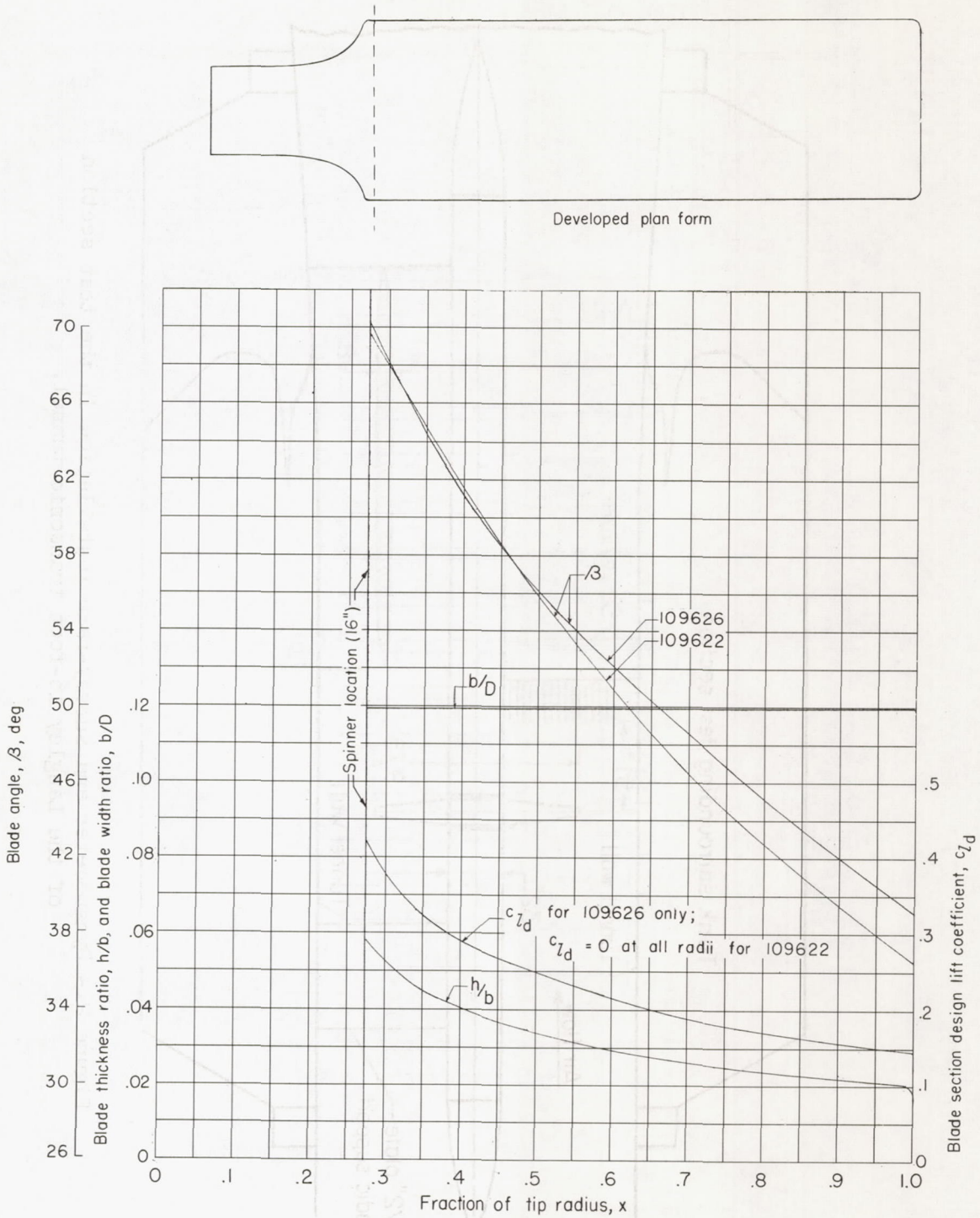


Figure 3.- Blade-form characteristics of two Curtiss-Wright supersonic propellers (design nos. 109622 and 109626).

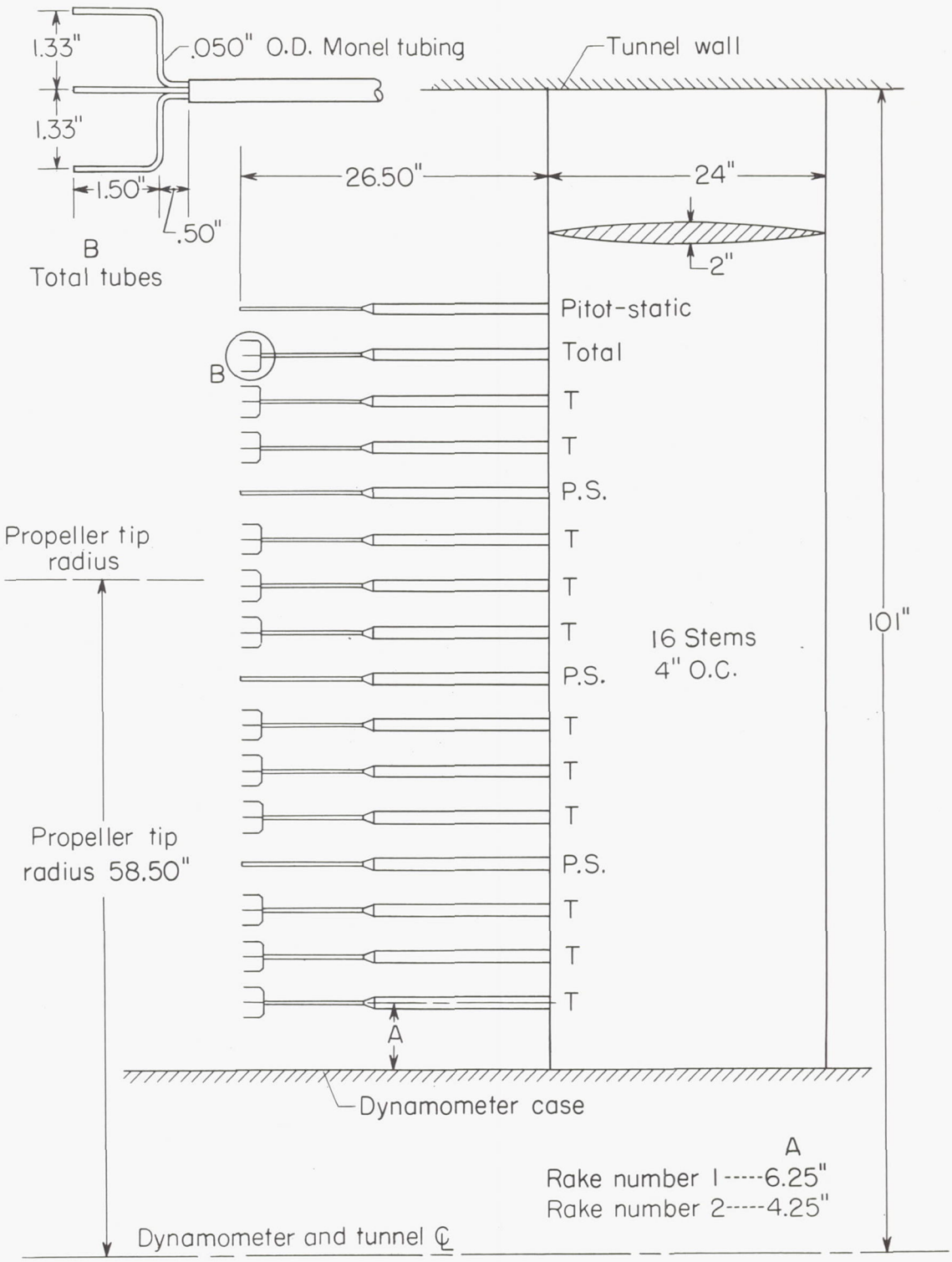
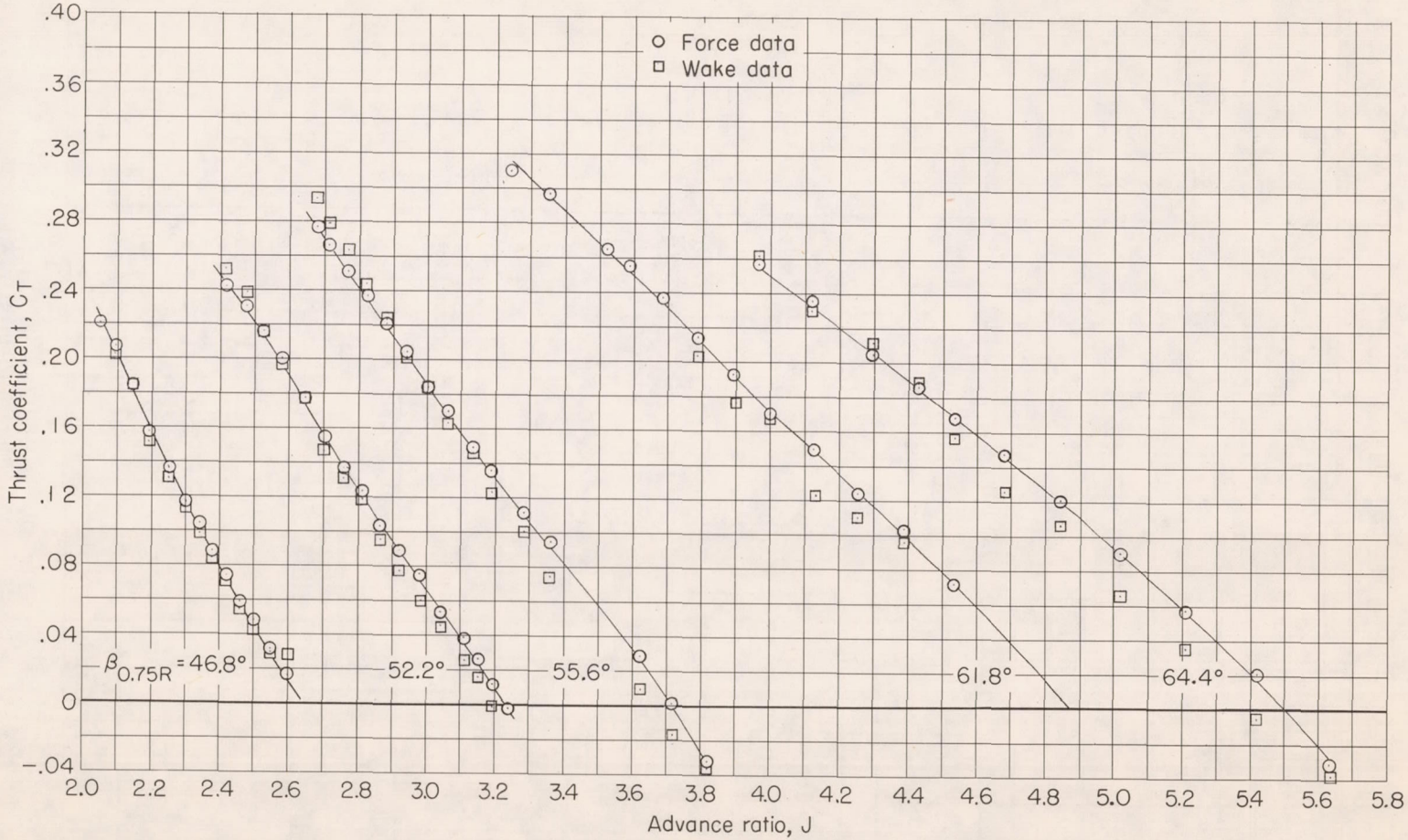
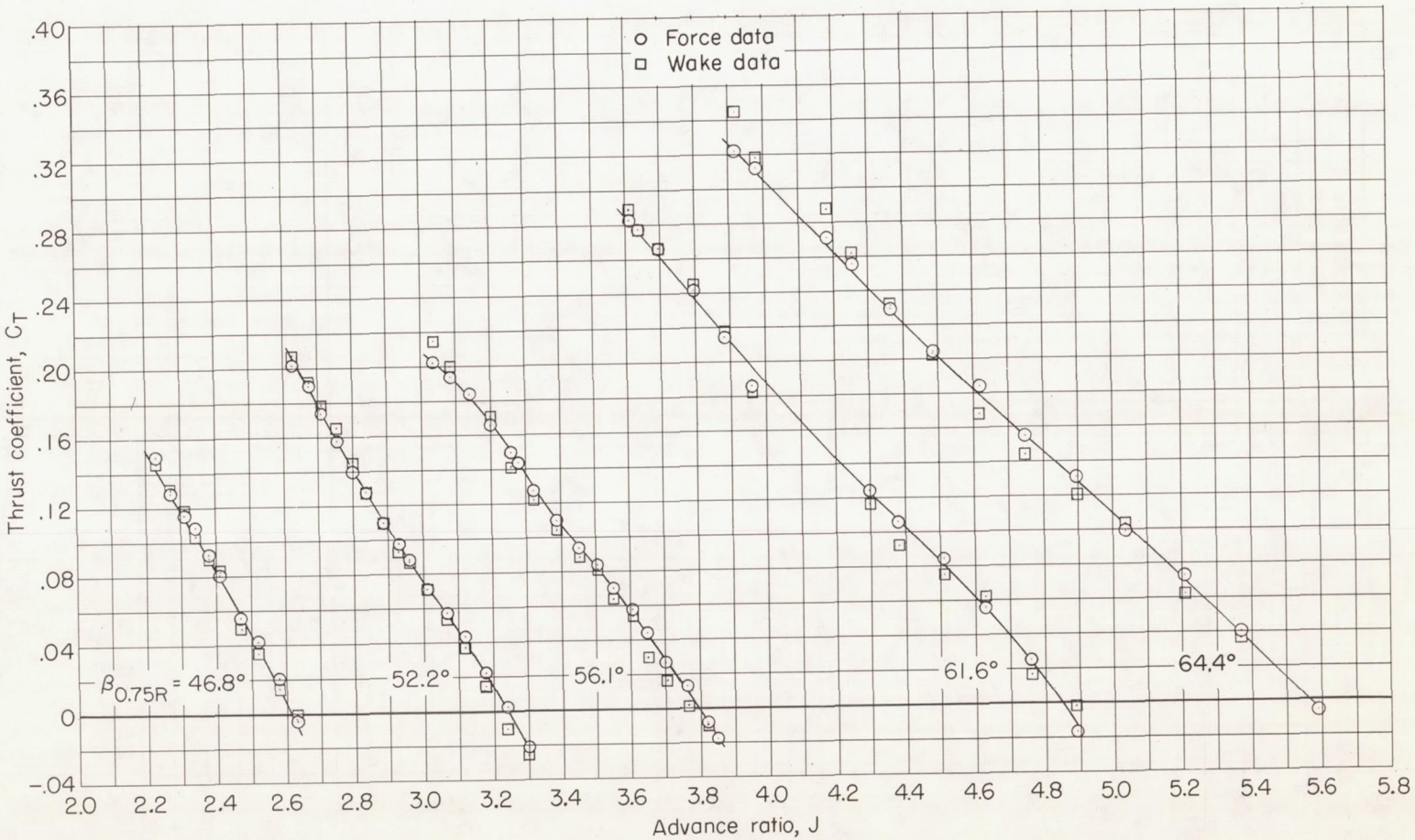


Figure 4.- Sketch of rake number 1. Rake number 2 is identical except in dimension A.



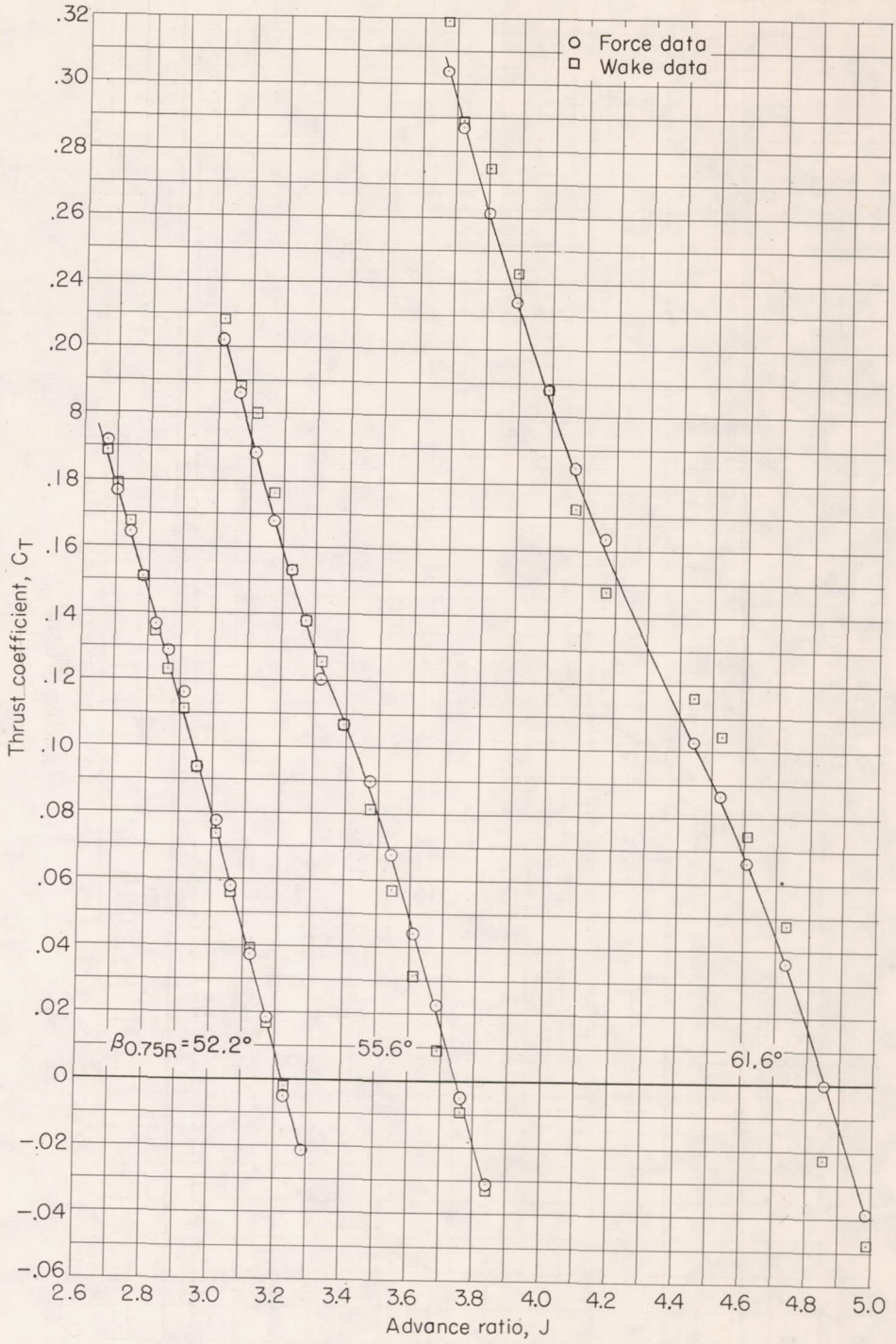
(a) M = 0.60.

Figure 5.- Comparison of the variation of integrated thrust coefficient and force test thrust coefficient with advance ratio. 109626 propeller.



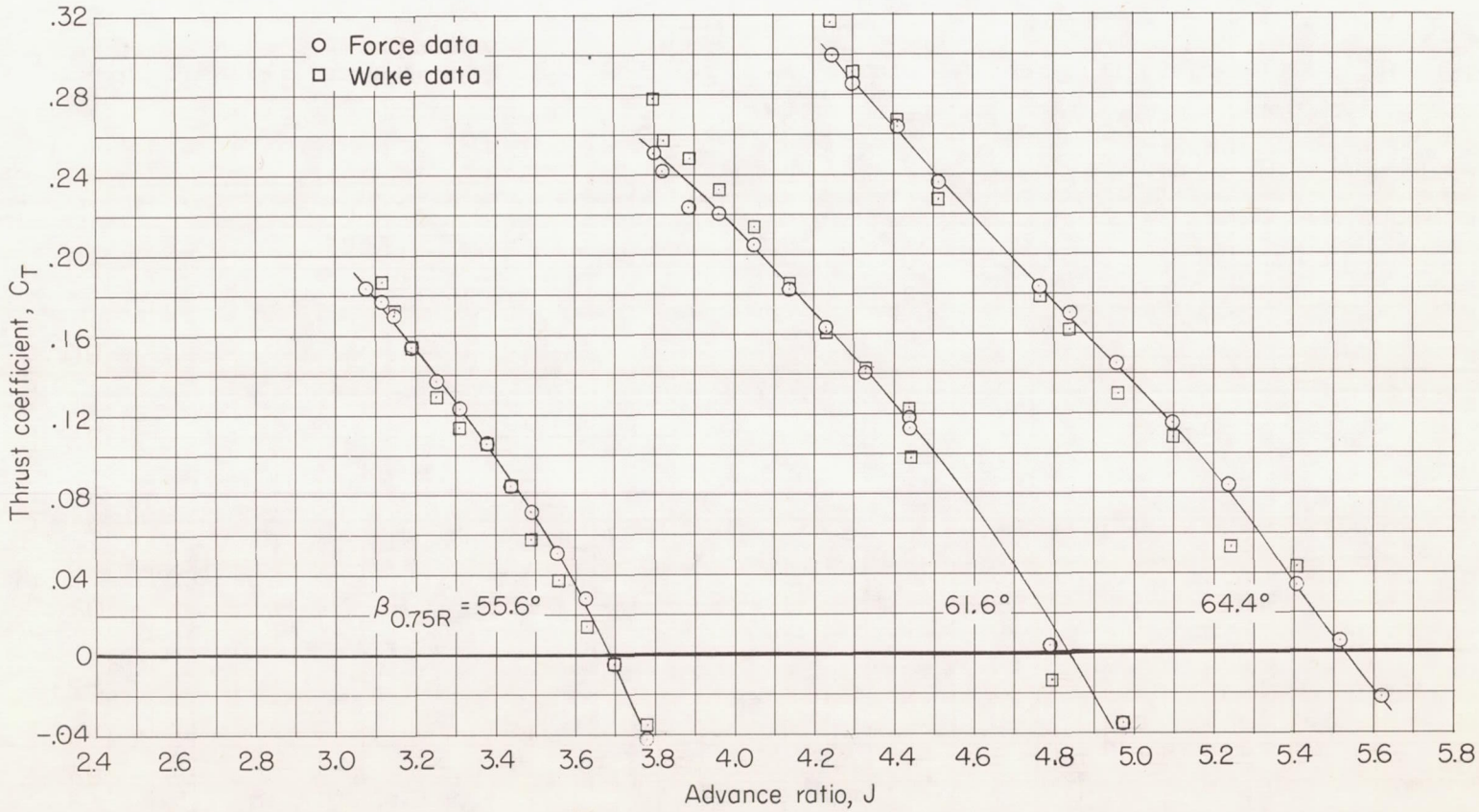
(b) M = 0.70.

Figure 5.- Continued.



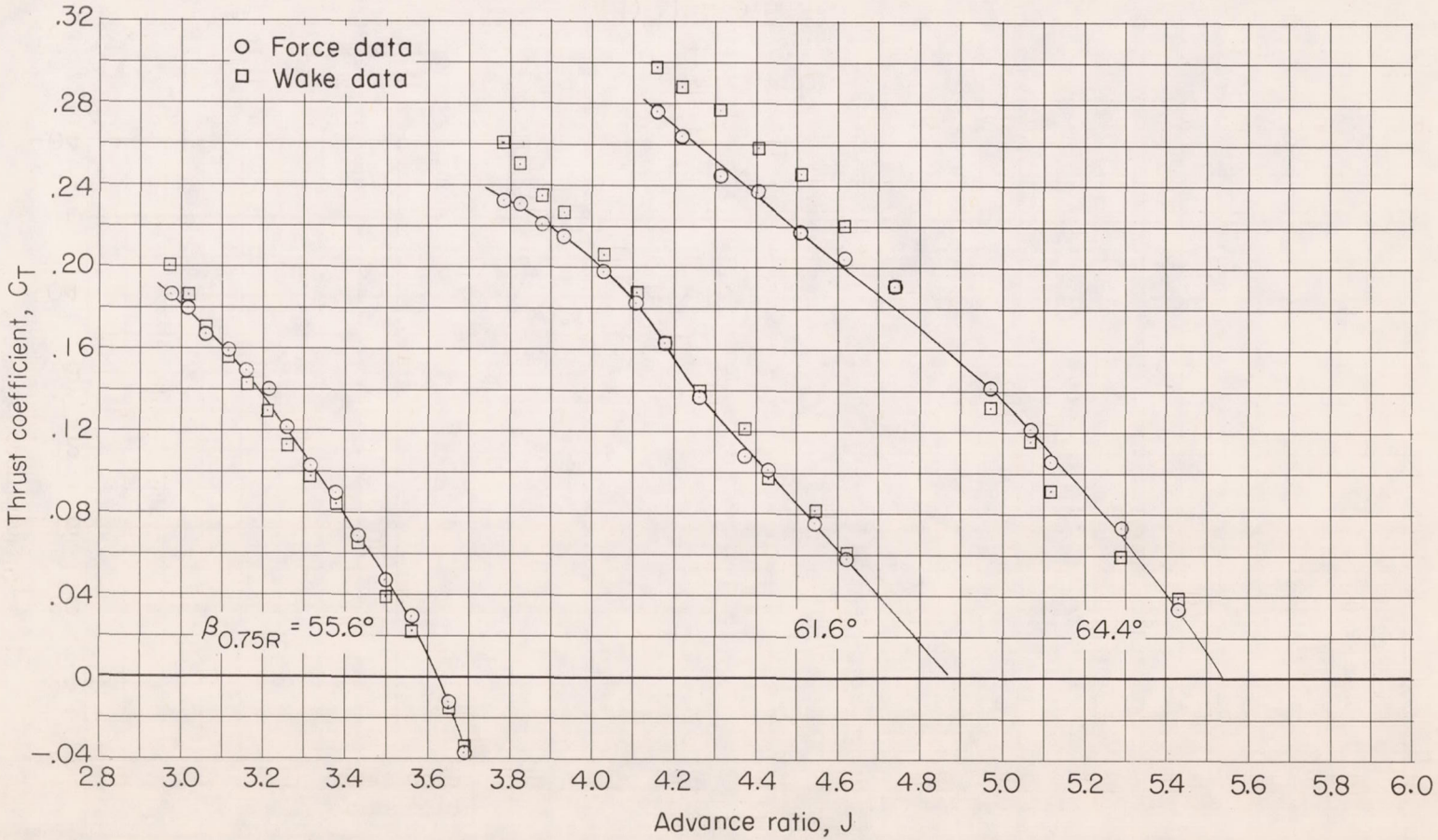
(c) M = 0.74.

Figure 5.- Continued.



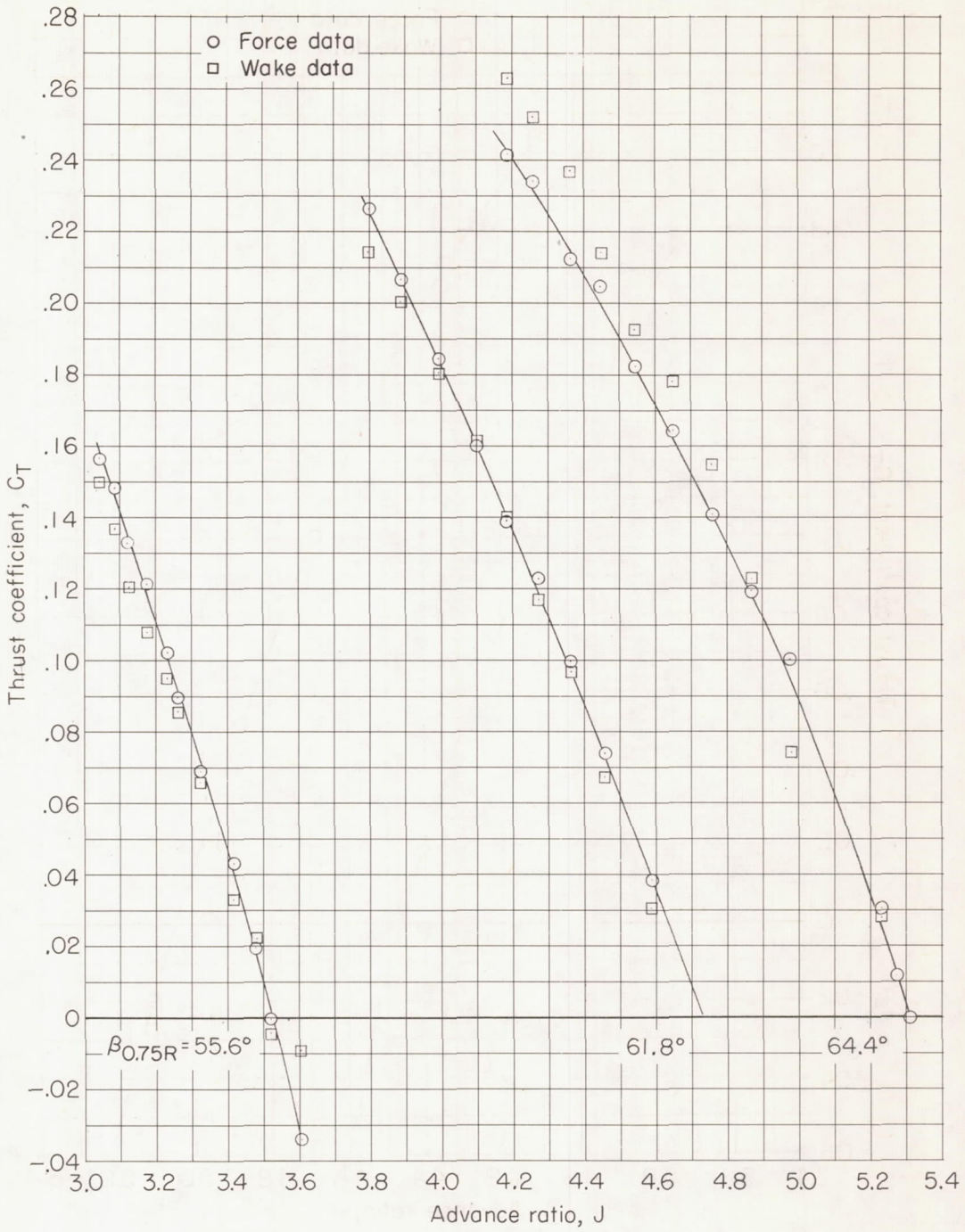
(d) M = 0.80.

Figure 5.- Continued.



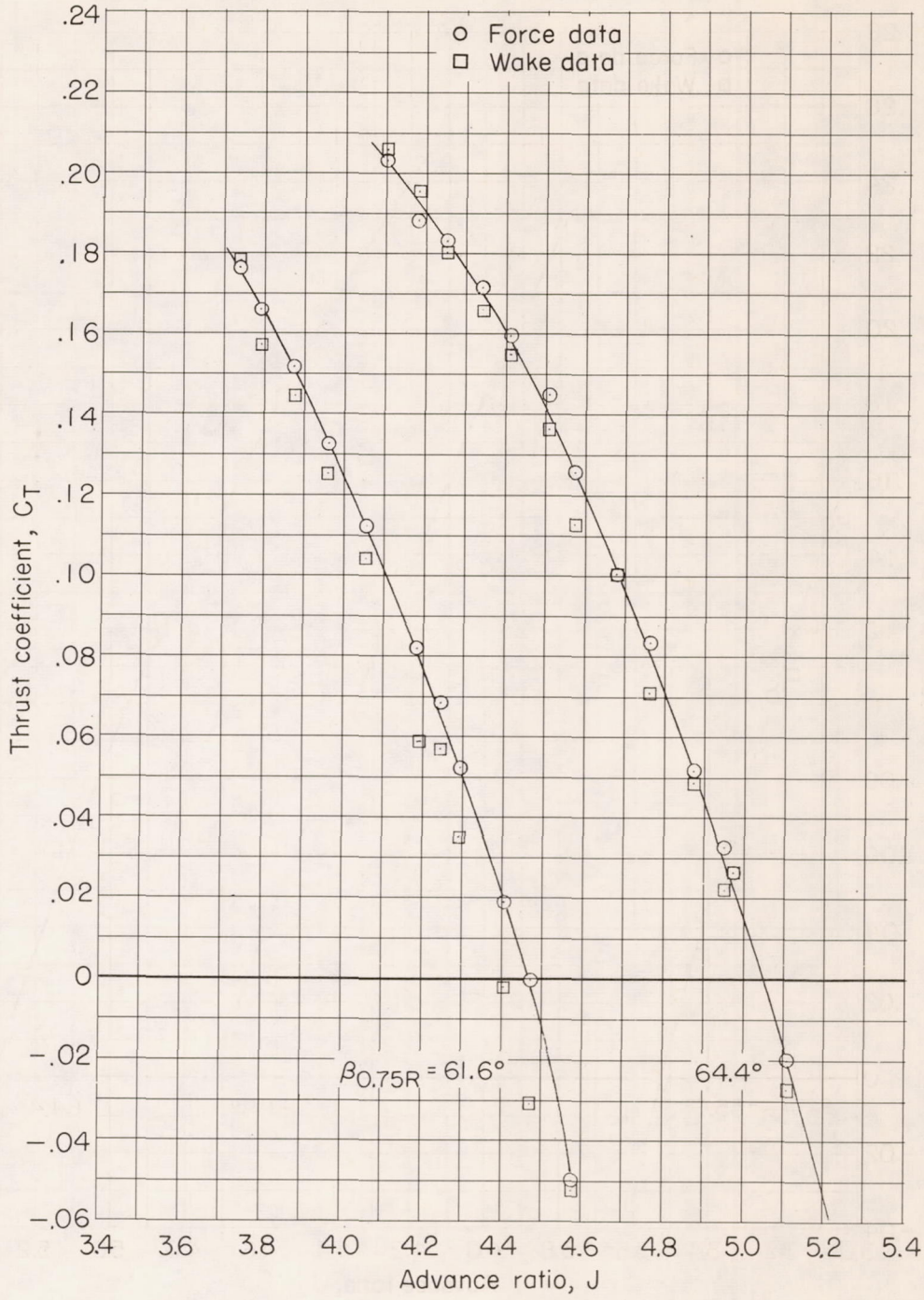
(e) M = 0.84.

Figure 5.- Continued.



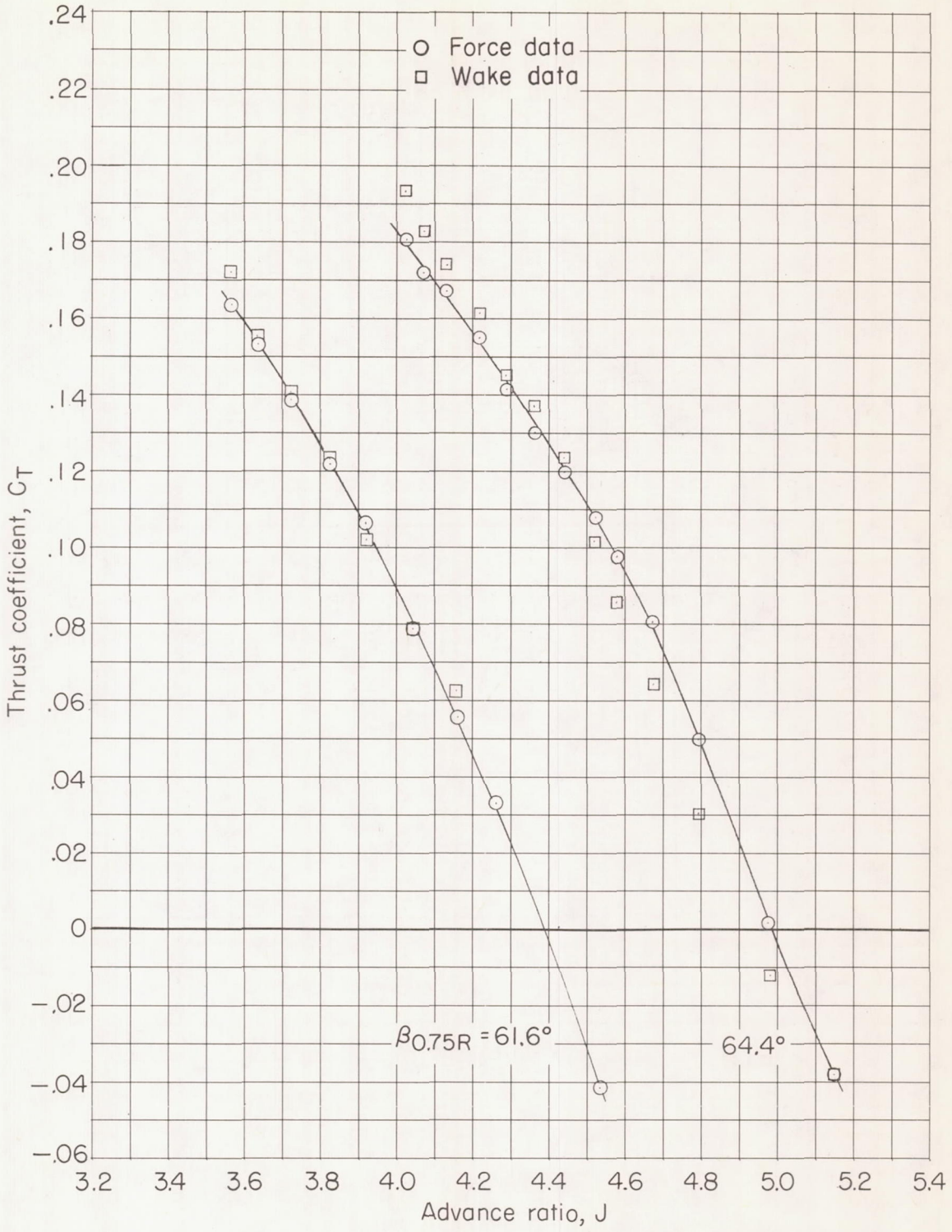
(f) M = 0.89.

Figure 5.- Continued.



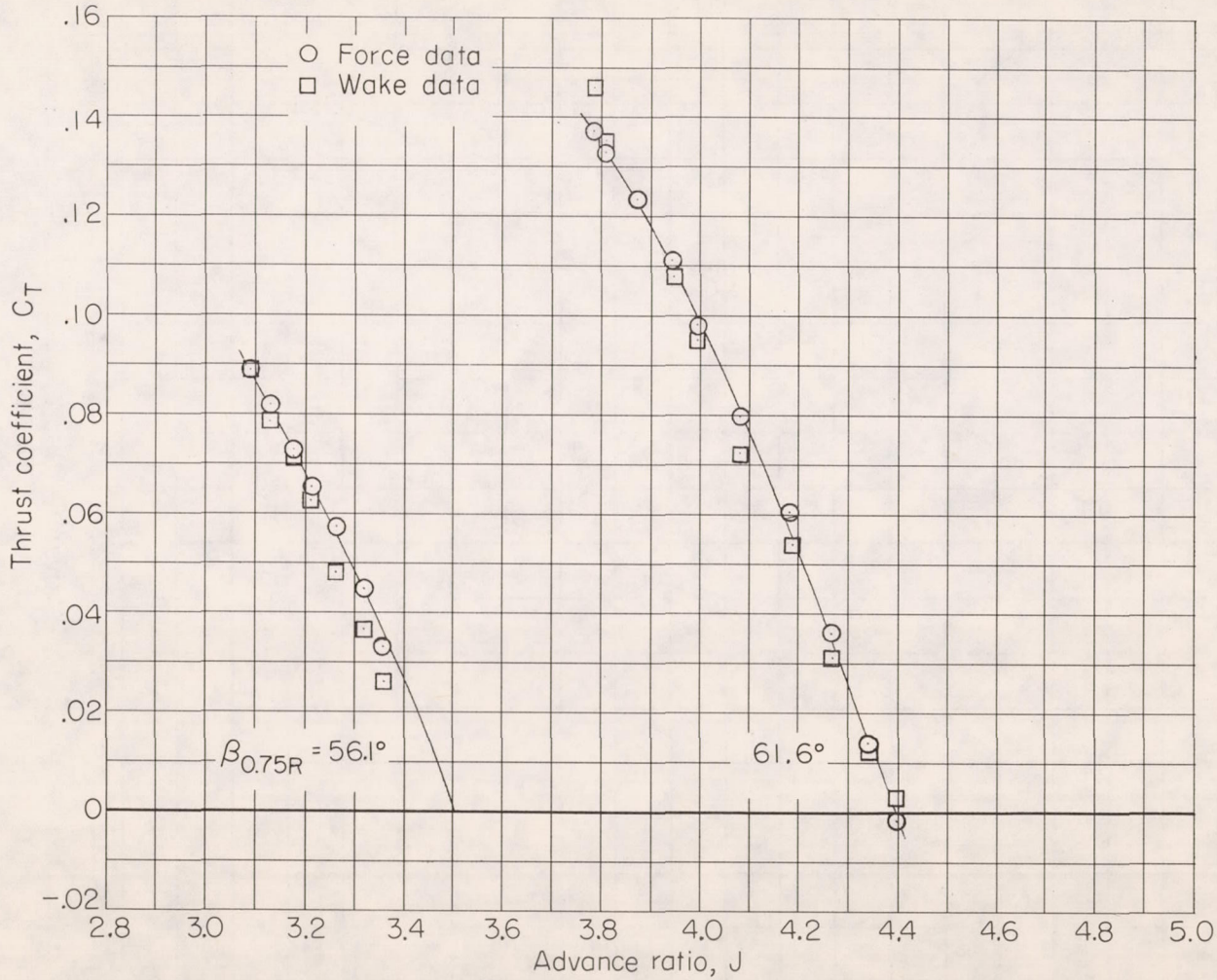
(g) M = 0.96.

Figure 5.- Continued.



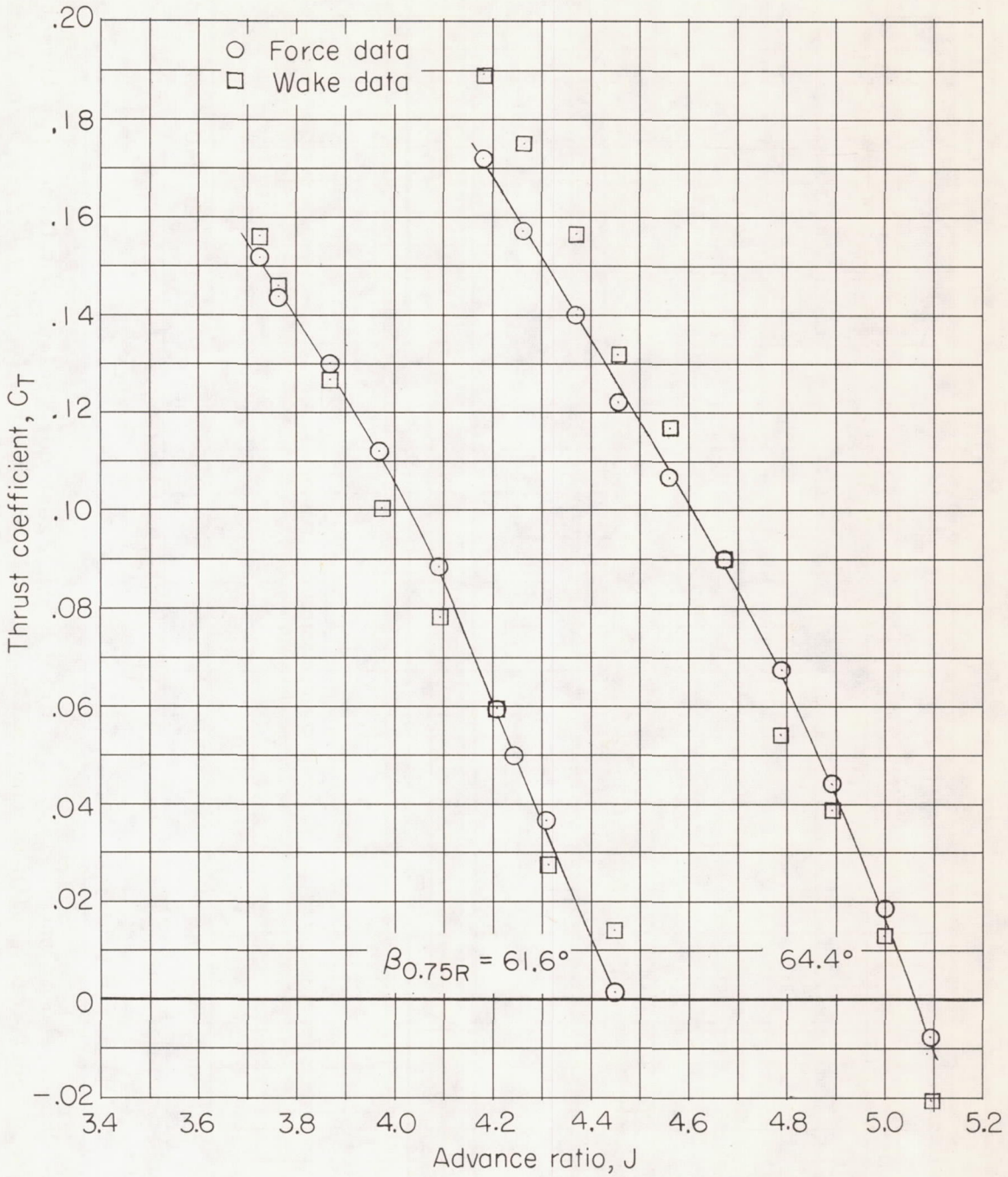
(h) M = 1.00.

Figure 5.- Continued.



(i) M = 1.02.

Figure 5.- Continued.



(j) M = 1.04.

Figure 5.- Concluded.

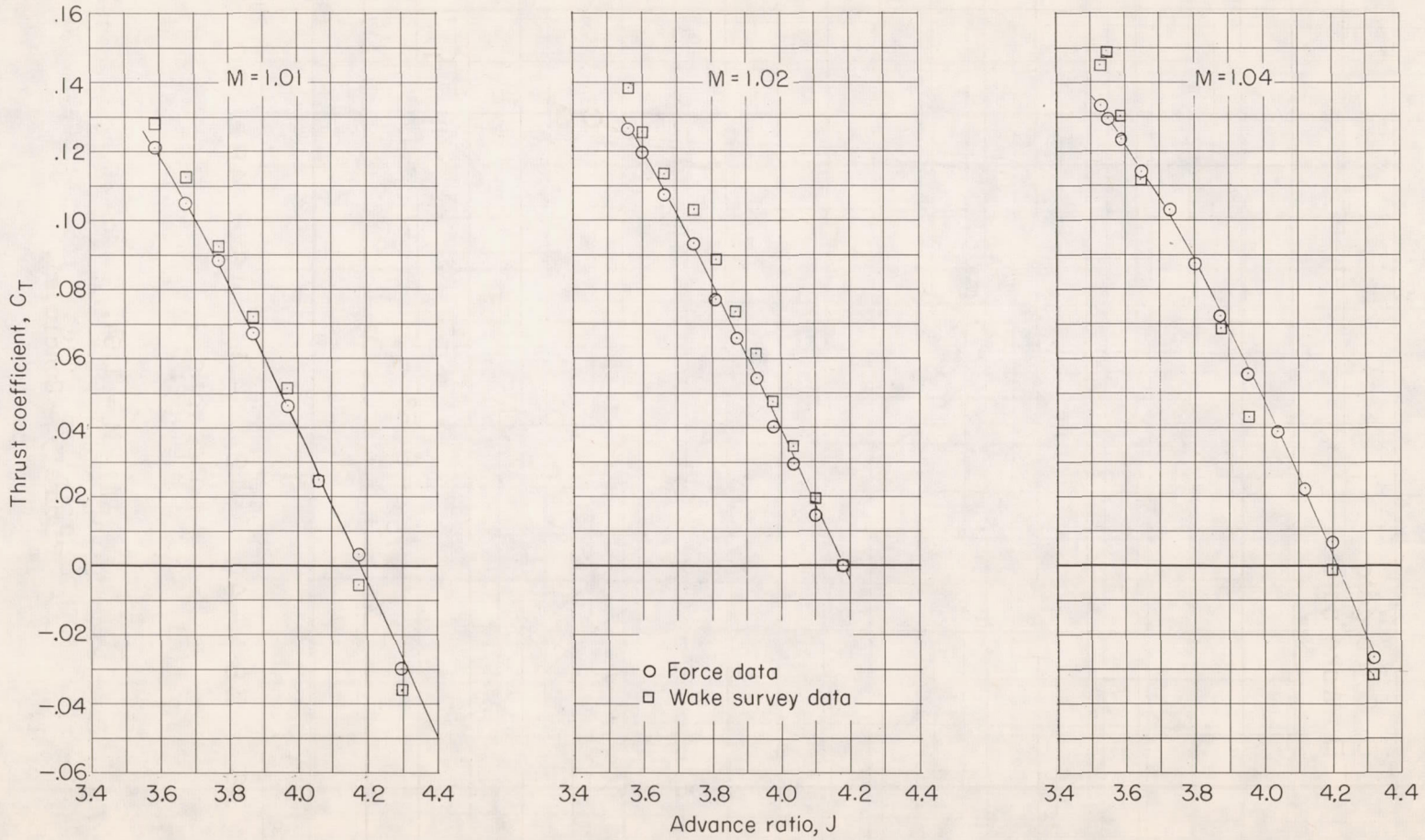
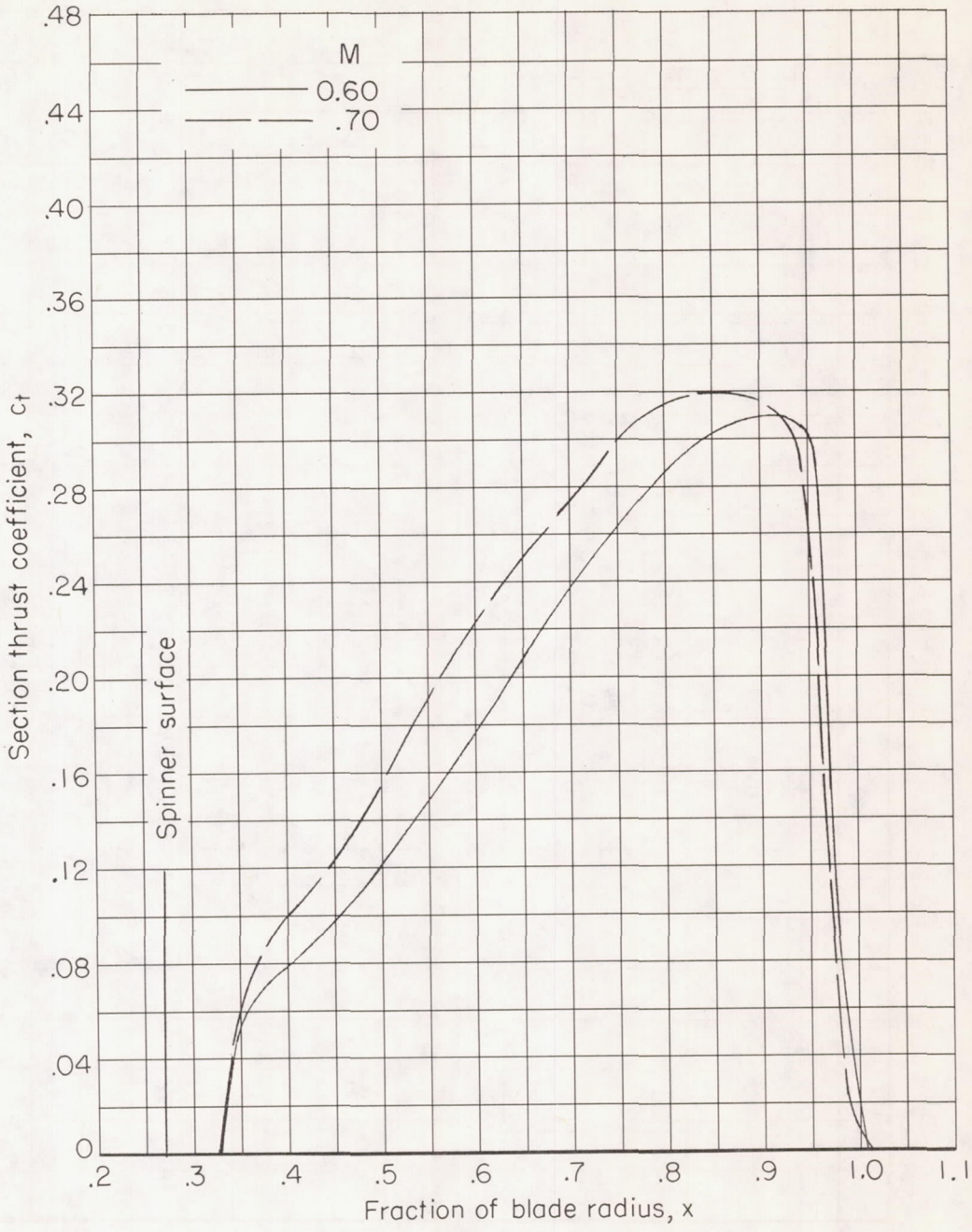
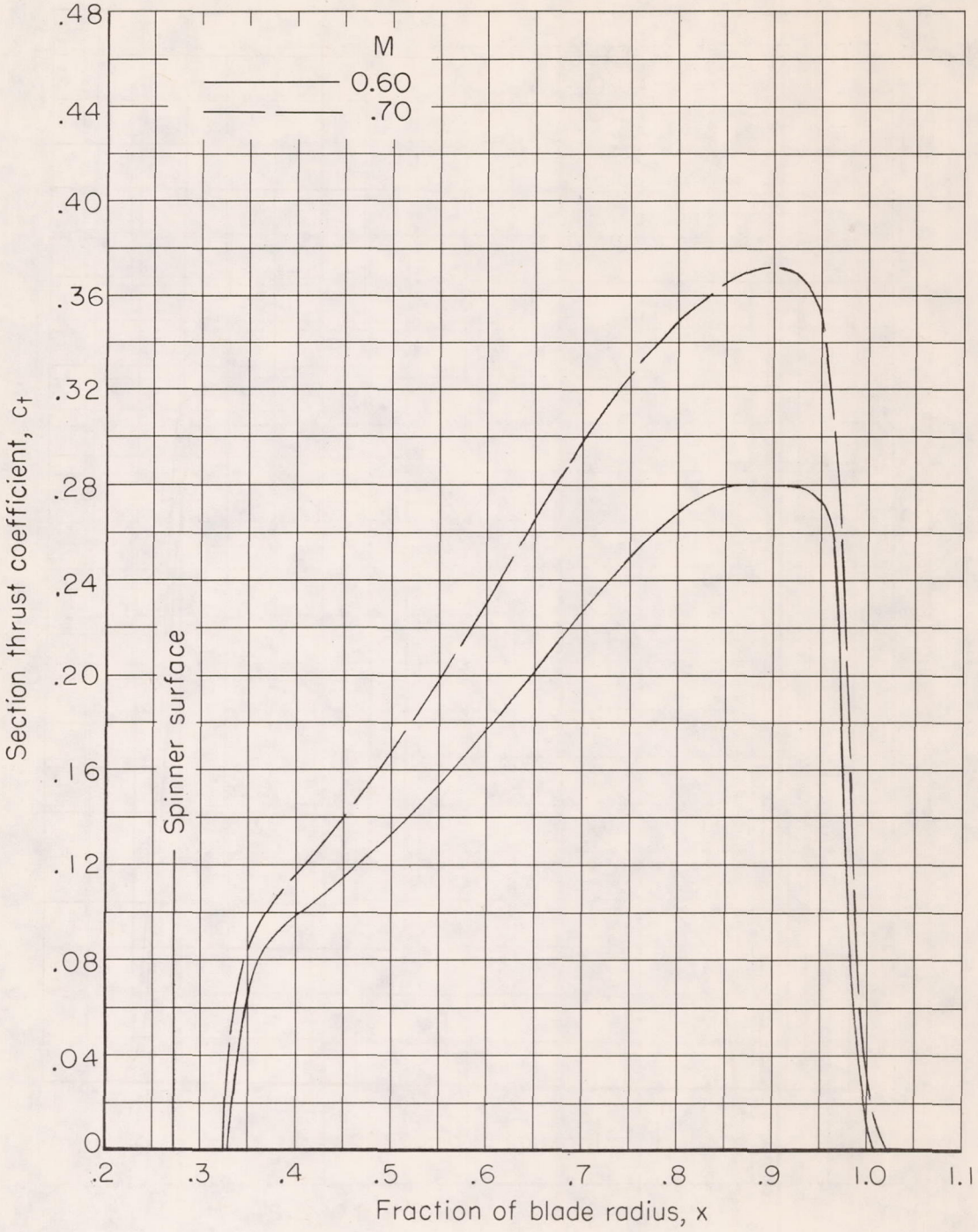


Figure 6.- Comparison of the variation of integrated thrust coefficient and force test thrust coefficient with advance ratio. 109622 propeller. $\beta_{0.75R} = 60^{\circ}$.



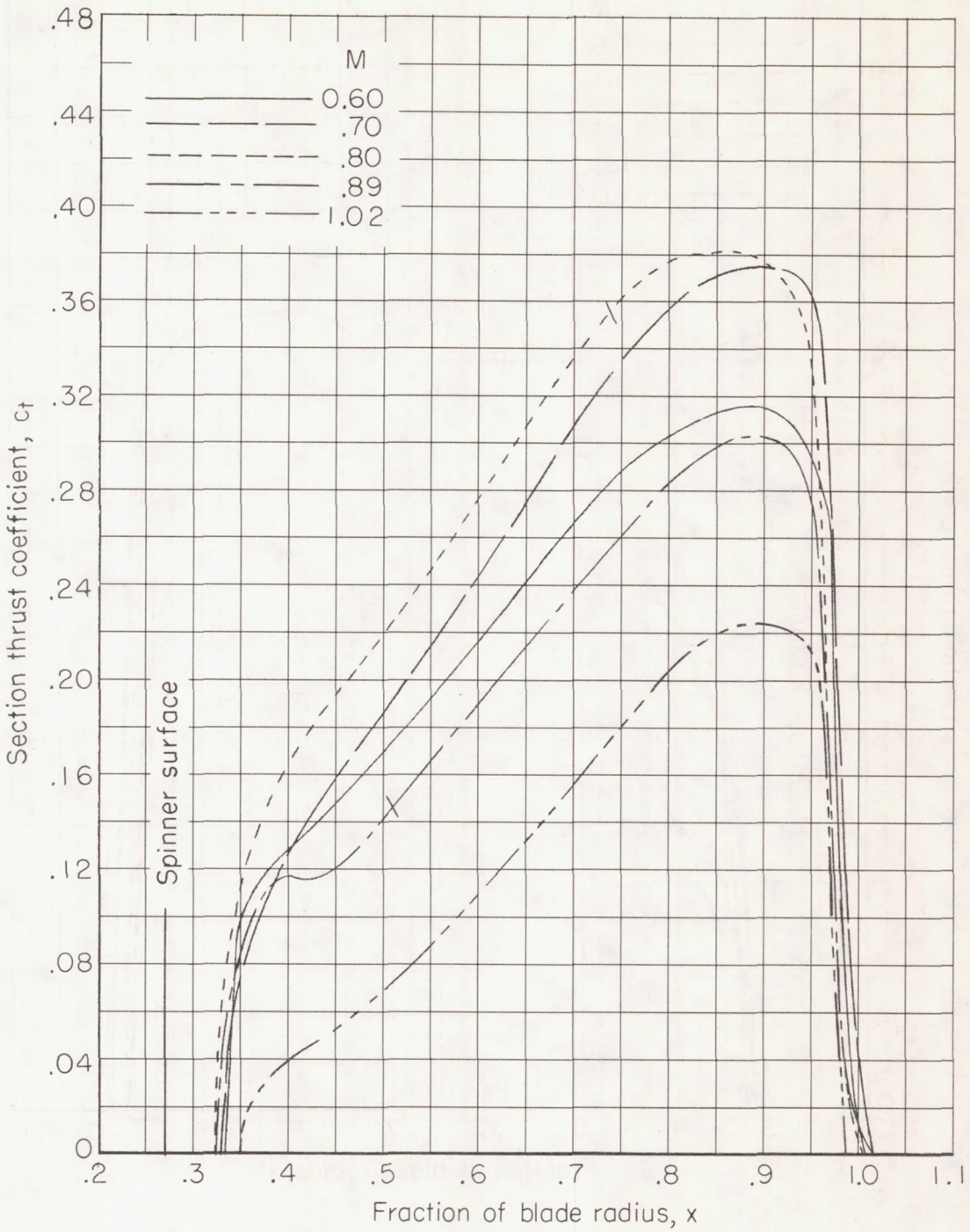
(a) $\beta_{0.75R} = 46.8^{\circ}$; J = 2.24.

Figure 7.- Thrust loading variation with Mach number for a constant advance ratio. 109626 propeller. Ticks indicate a section Mach number of 1.00.



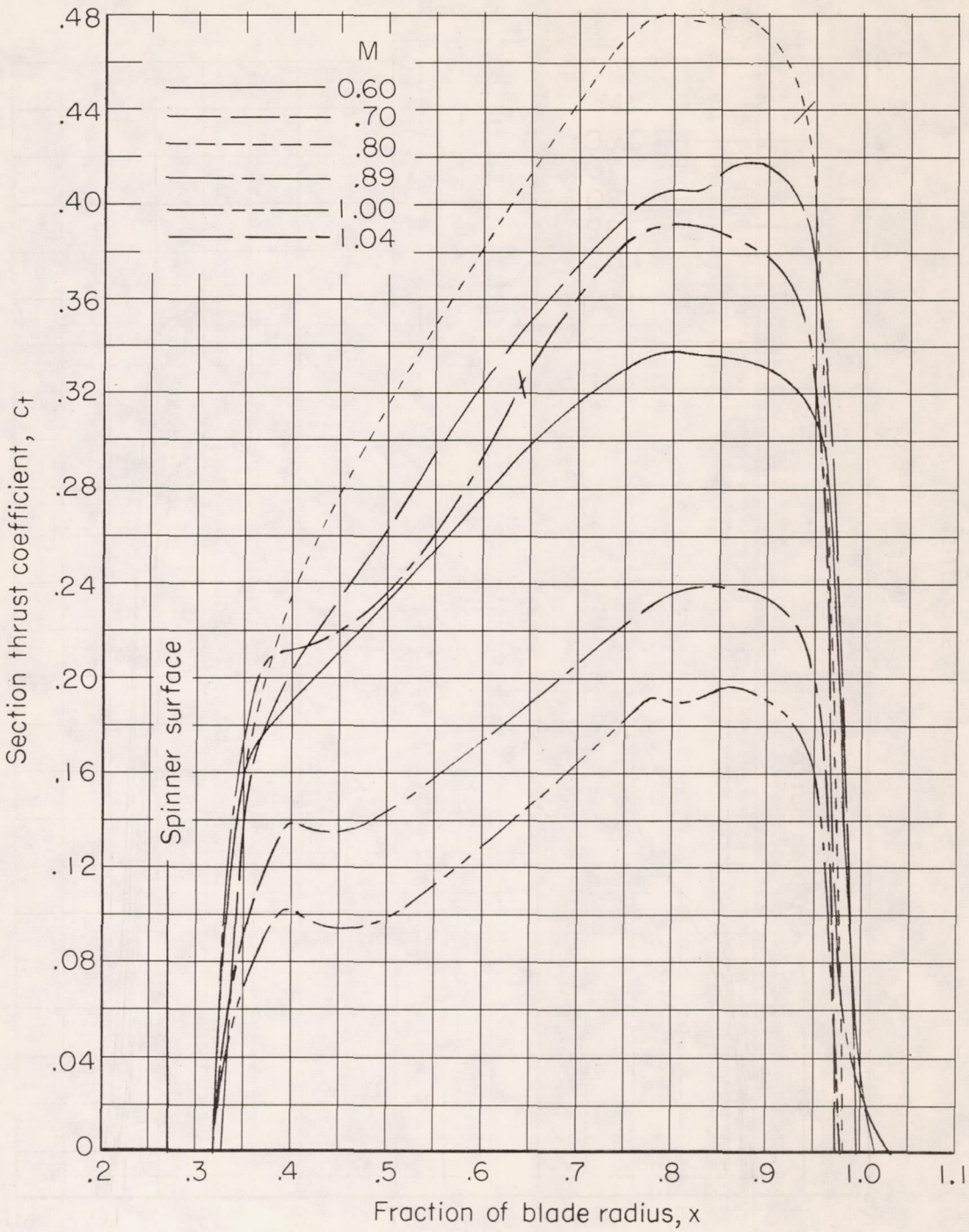
(b) $\beta_{0.75R} = 52.2^{\circ}$; J = 2.75.

Figure 7.- Continued.



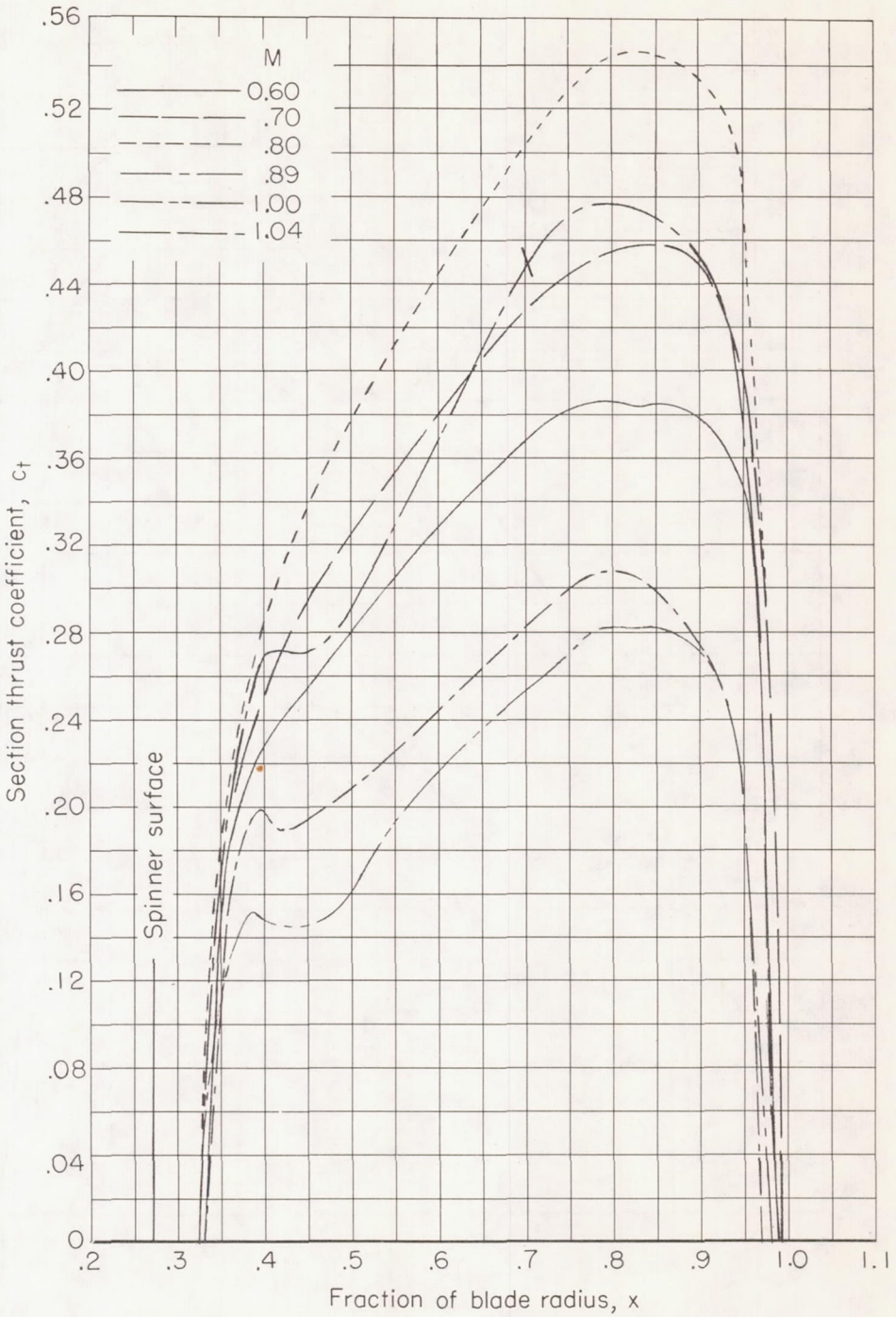
(c) $\beta_{0.75R} = 55.6°$; J = 3.10.

Figure 7.- Continued.



(d) $\beta_{0.75R} = 61.6°$; $J = 3.90$.

Figure 7.- Continued.



(e) $\beta_{0.75R} = 64.4^{\circ}$; J = 4.30.

Figure 7.- Concluded.

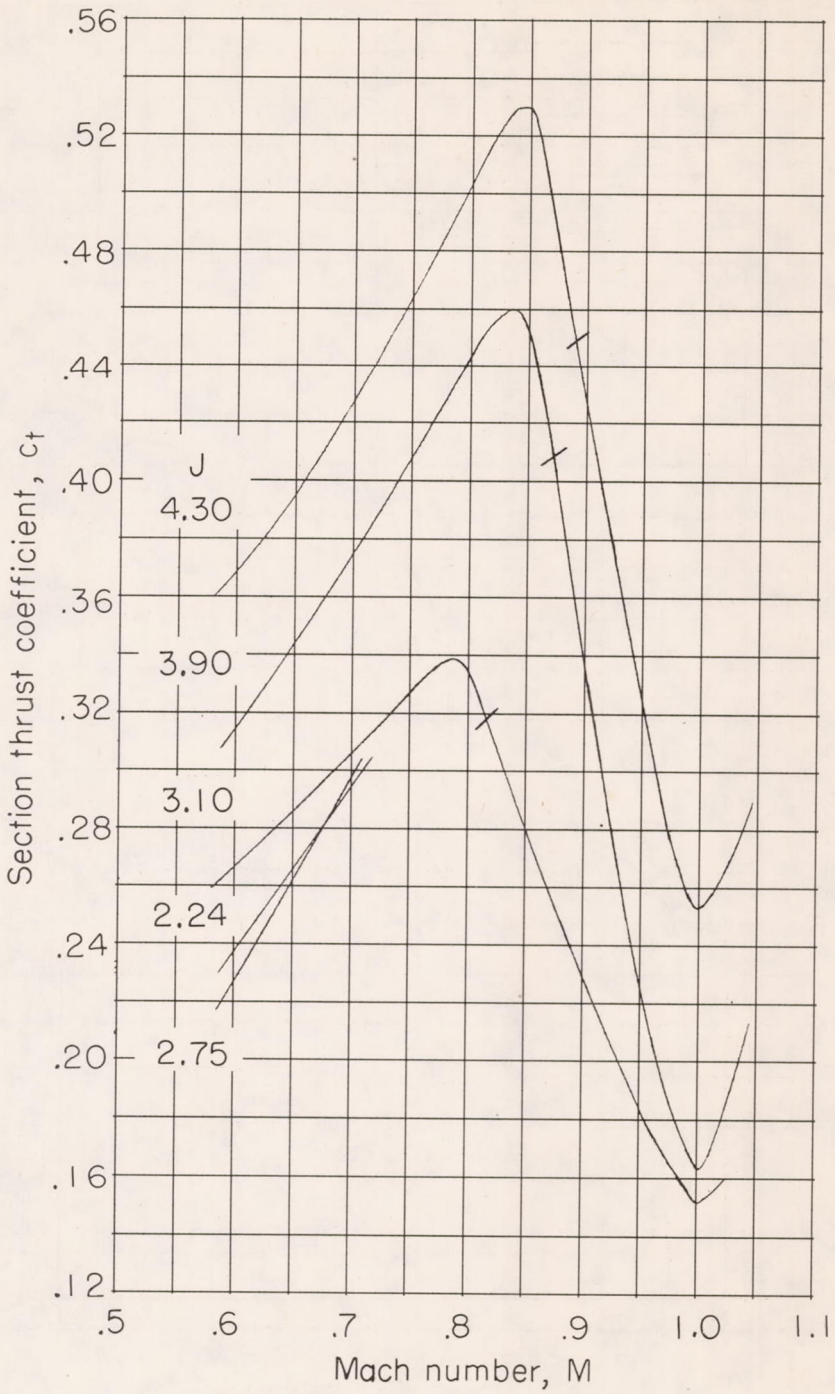


Figure 8.- Variation of section thrust coefficient at a typical radial station (x = 0.70) with free-stream Mach number for several values of advance ratio. Ticks indicate a section Mach number of 1.00.

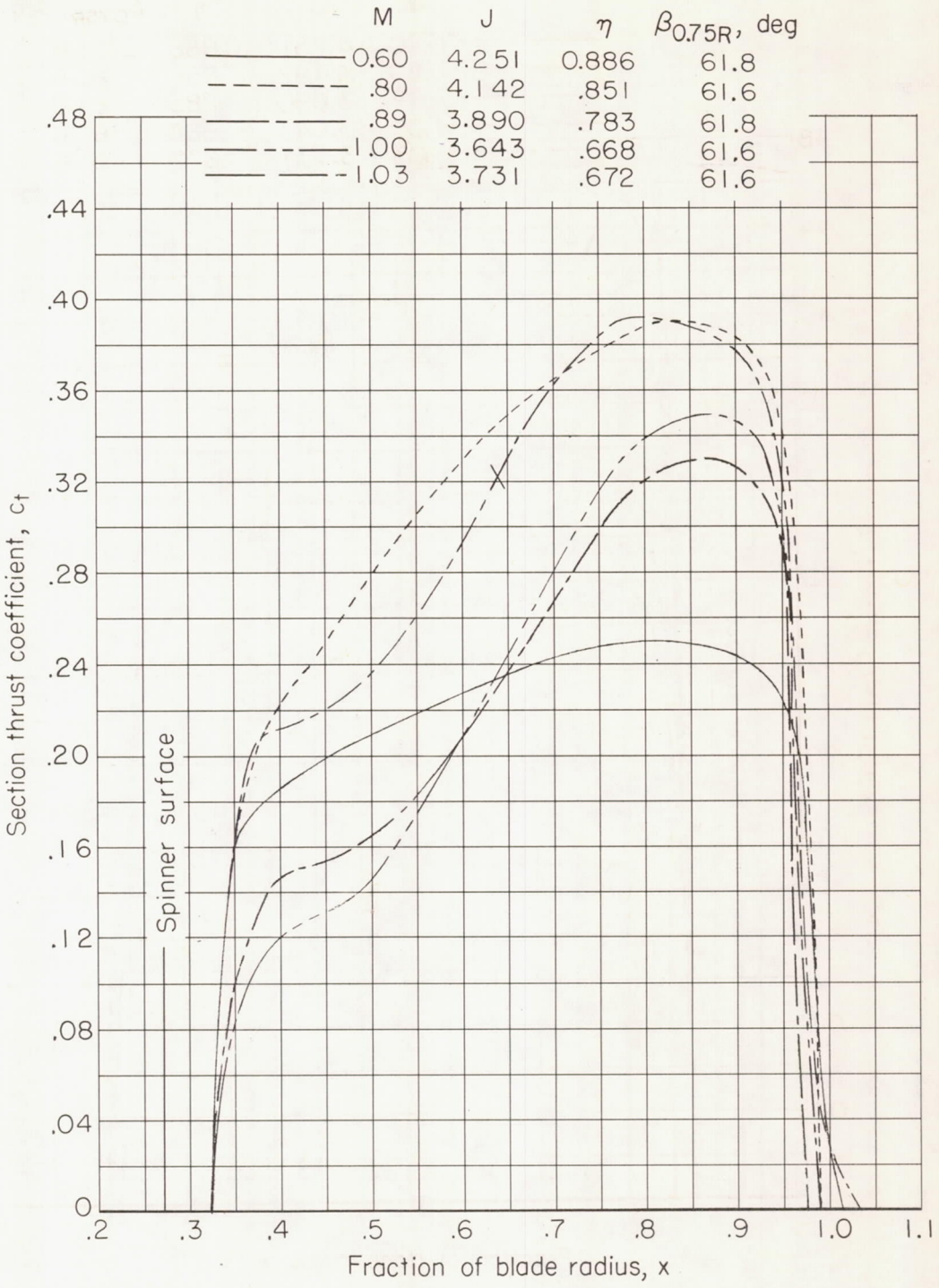


Figure 9.- Thrust loading variation with Mach number at advance ratio for maximum efficiency. 109626 propeller.

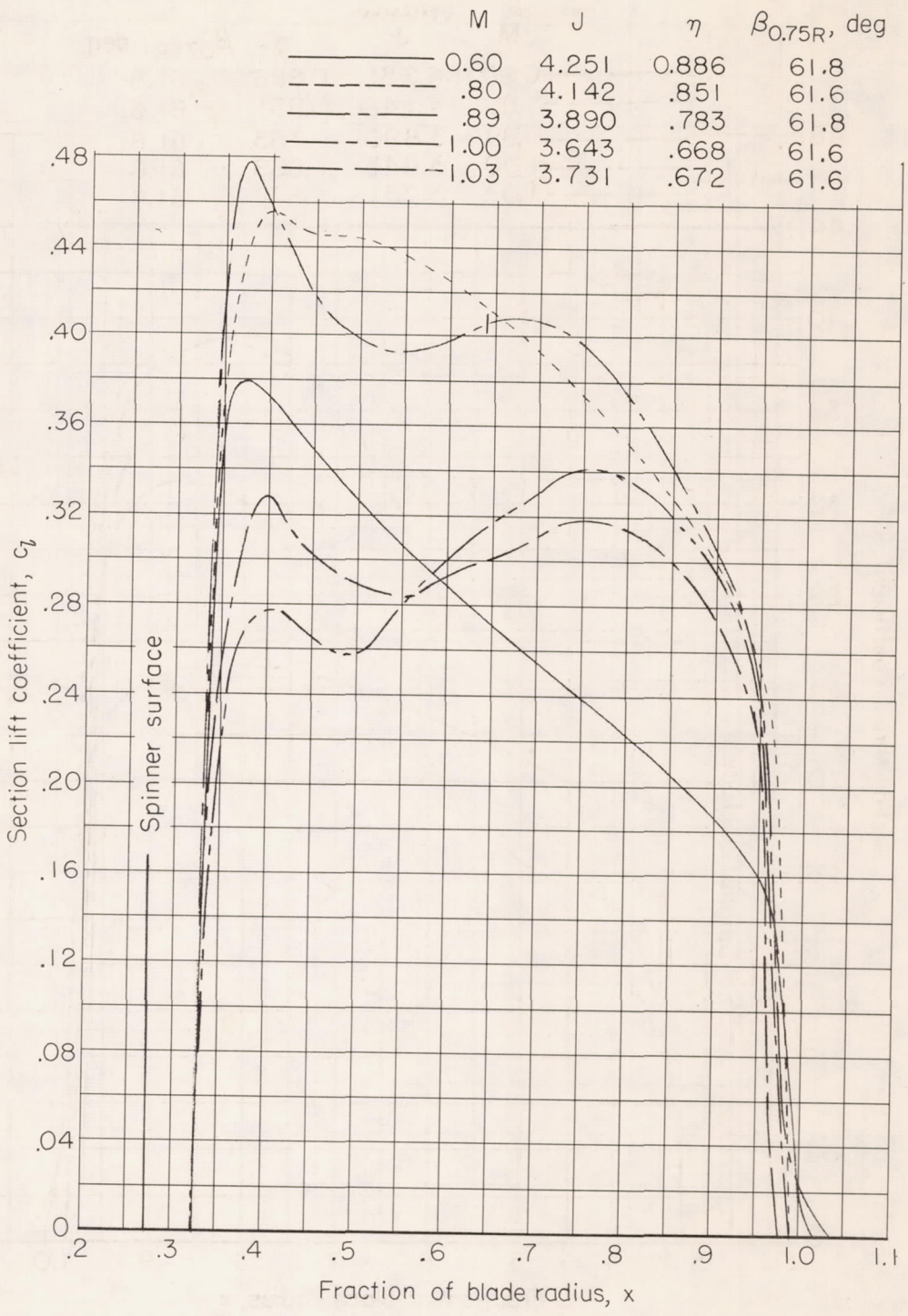


Figure 10.- Lift loading variation with Mach number and advance ratios for maximum efficiency. 109626 propeller.

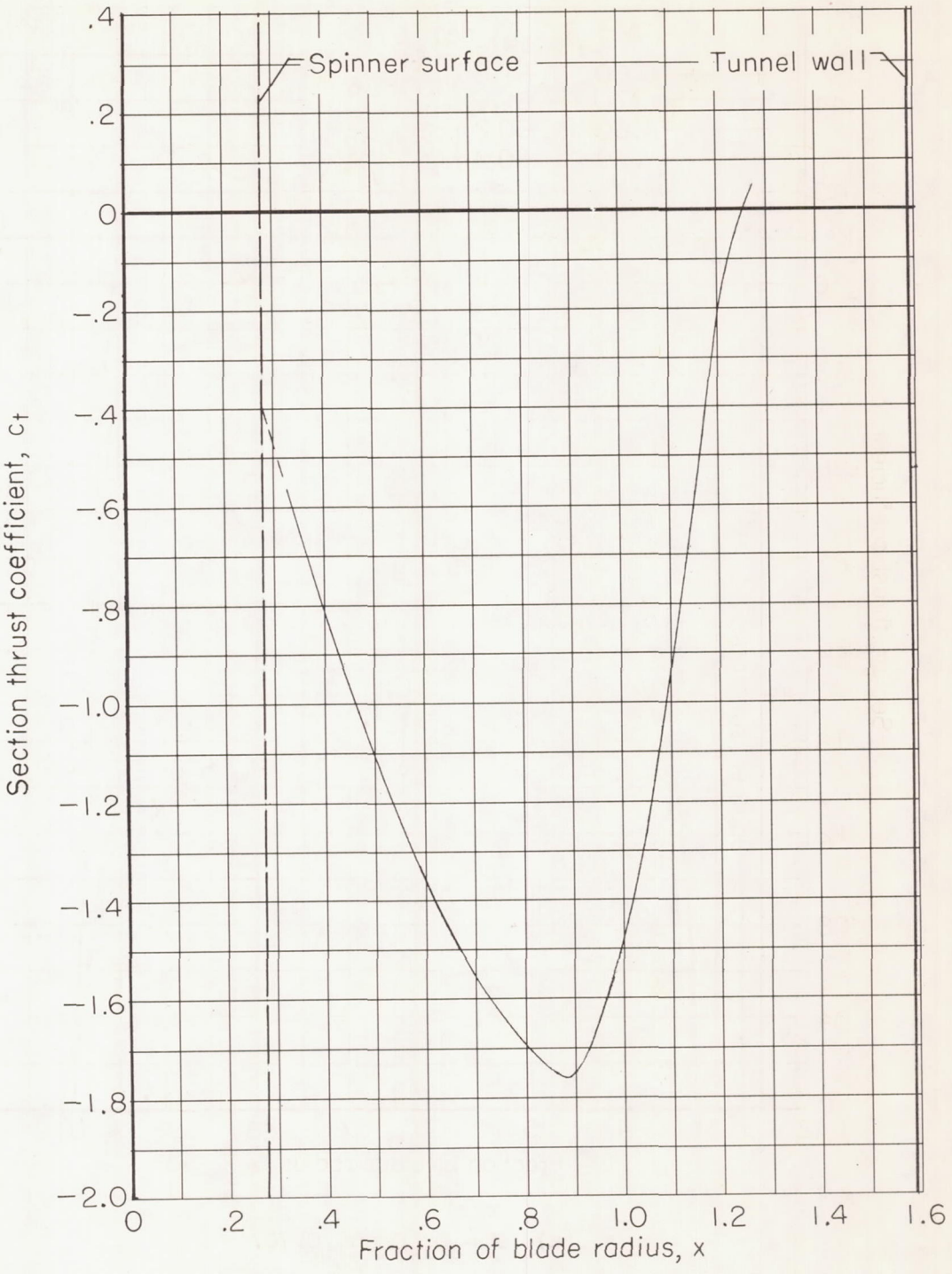
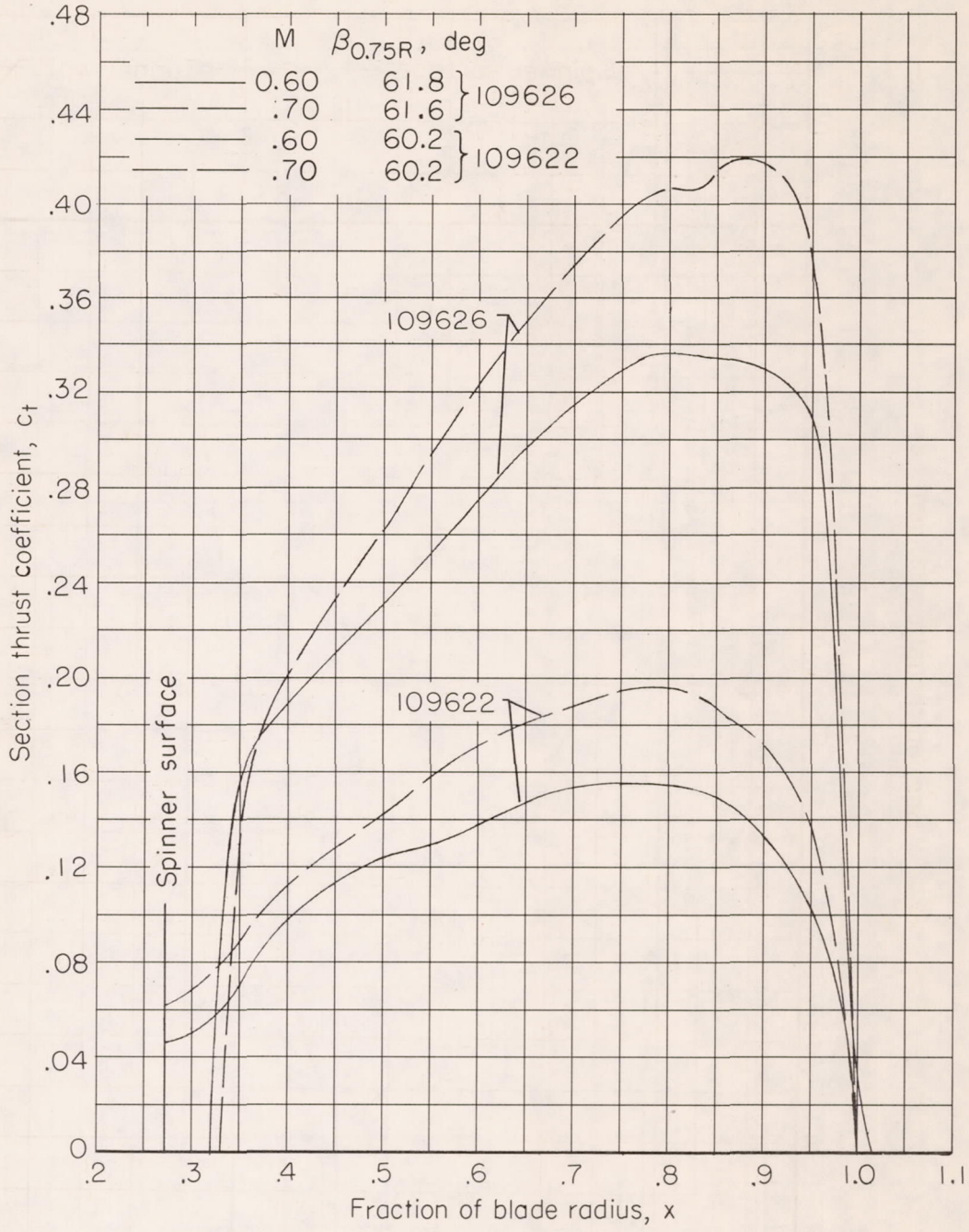
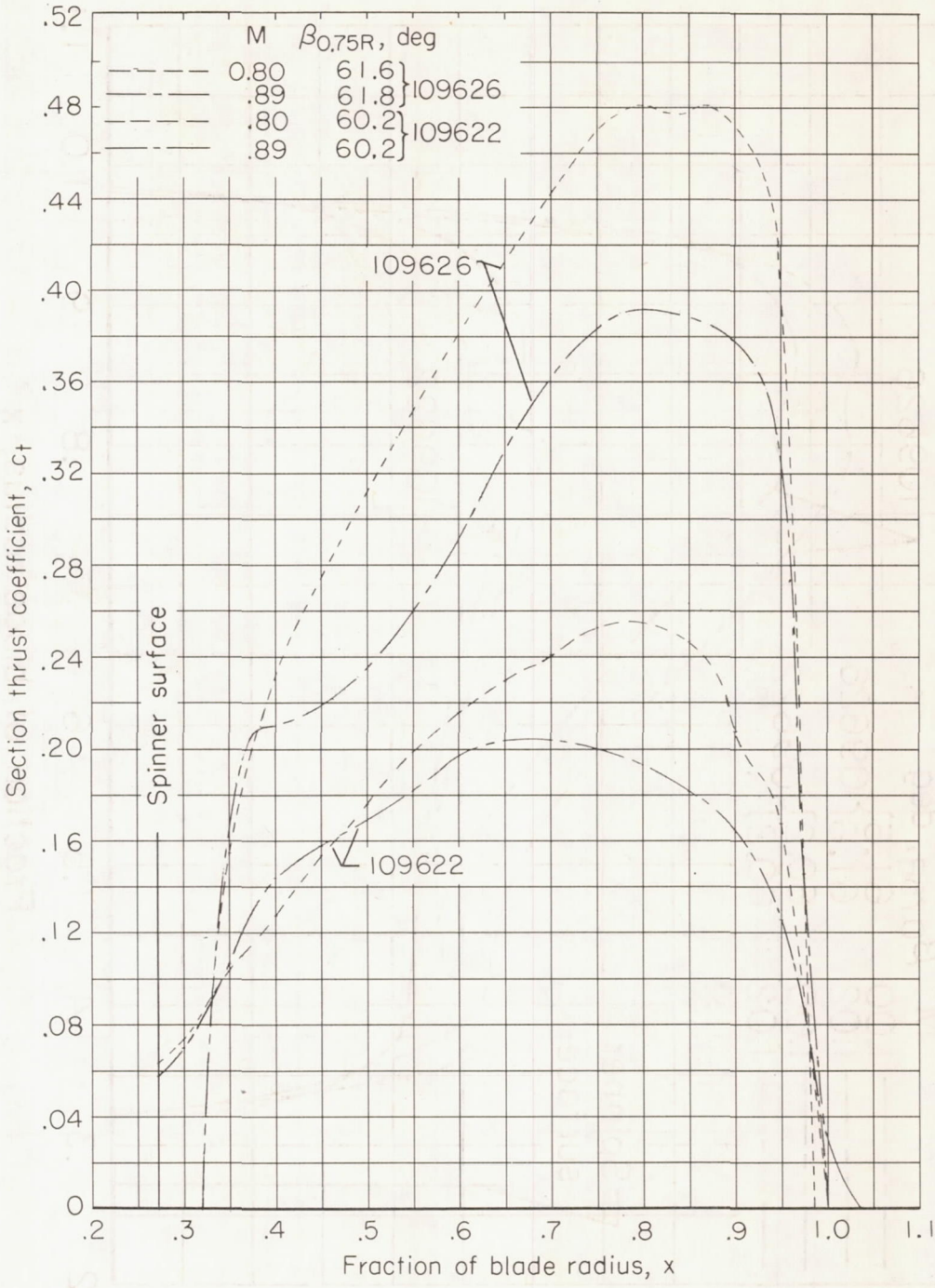


Figure 11.- Typical thrust loading curve for negative blade angles. 109626 propeller; $\beta_{0.75R} = -13.6^{\circ}$; M = 0.13; 650 rpm.



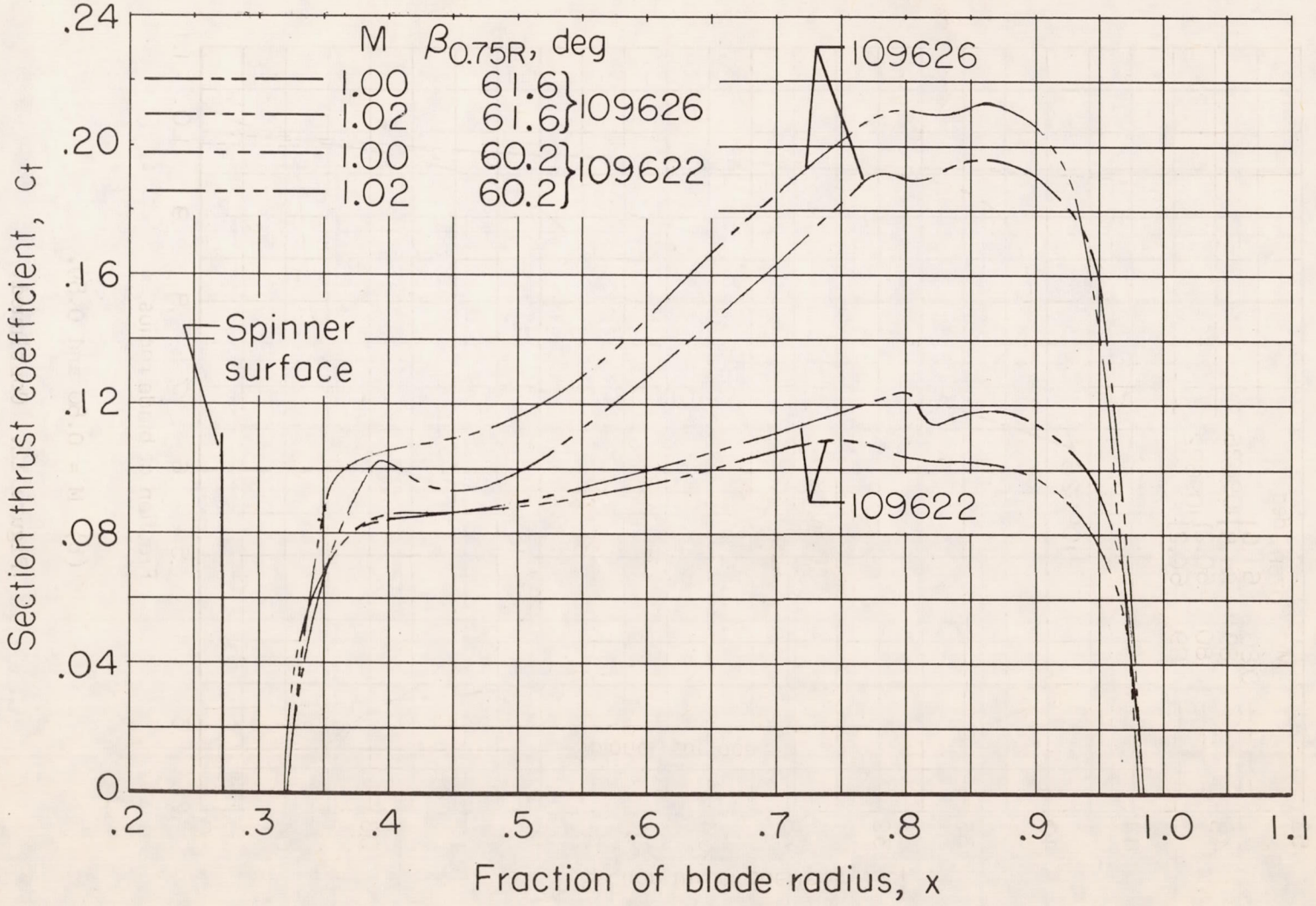
(a) M = 0.60 and 0.70.

Figure 12.- Section thrust loading comparisons between 109622 and 109626 propellers at advance ratio 3.90.



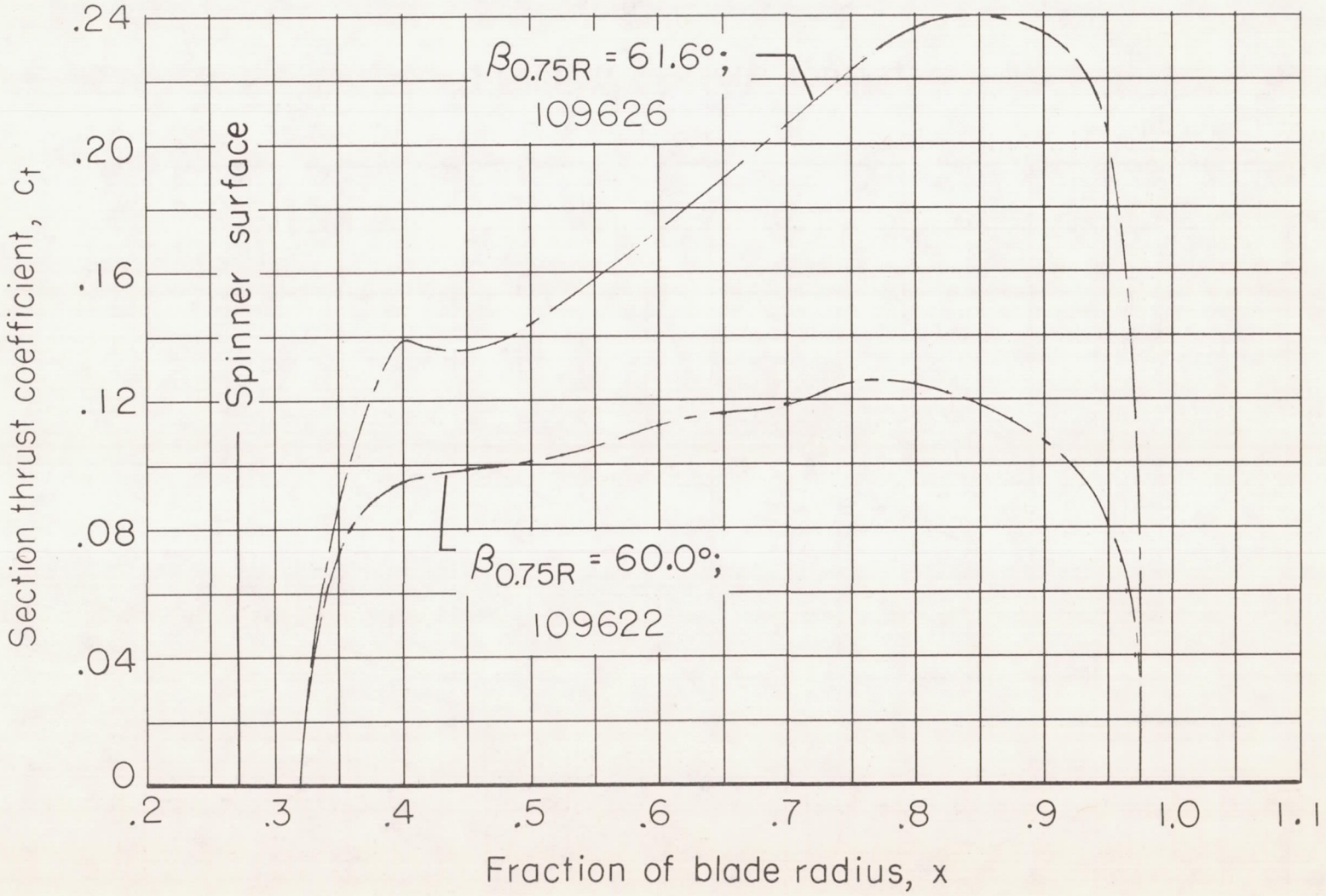
(b) M = 0.80 and 0.89.

Figure 12.- Continued.



(c) M = 1.00 and 1.02.

Figure 12.- Continued.



(d) M = 1.04.

Figure 12.- Concluded.

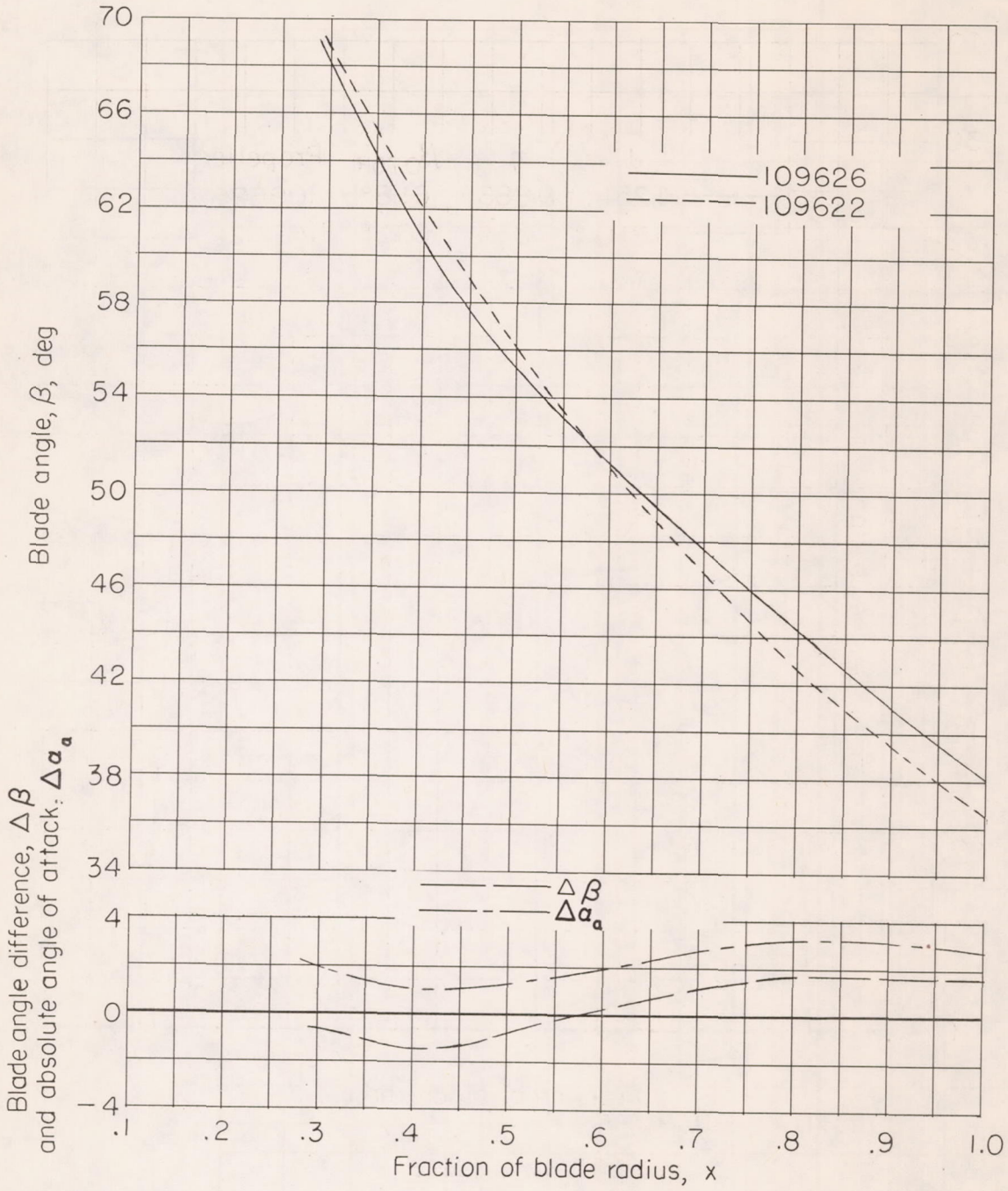
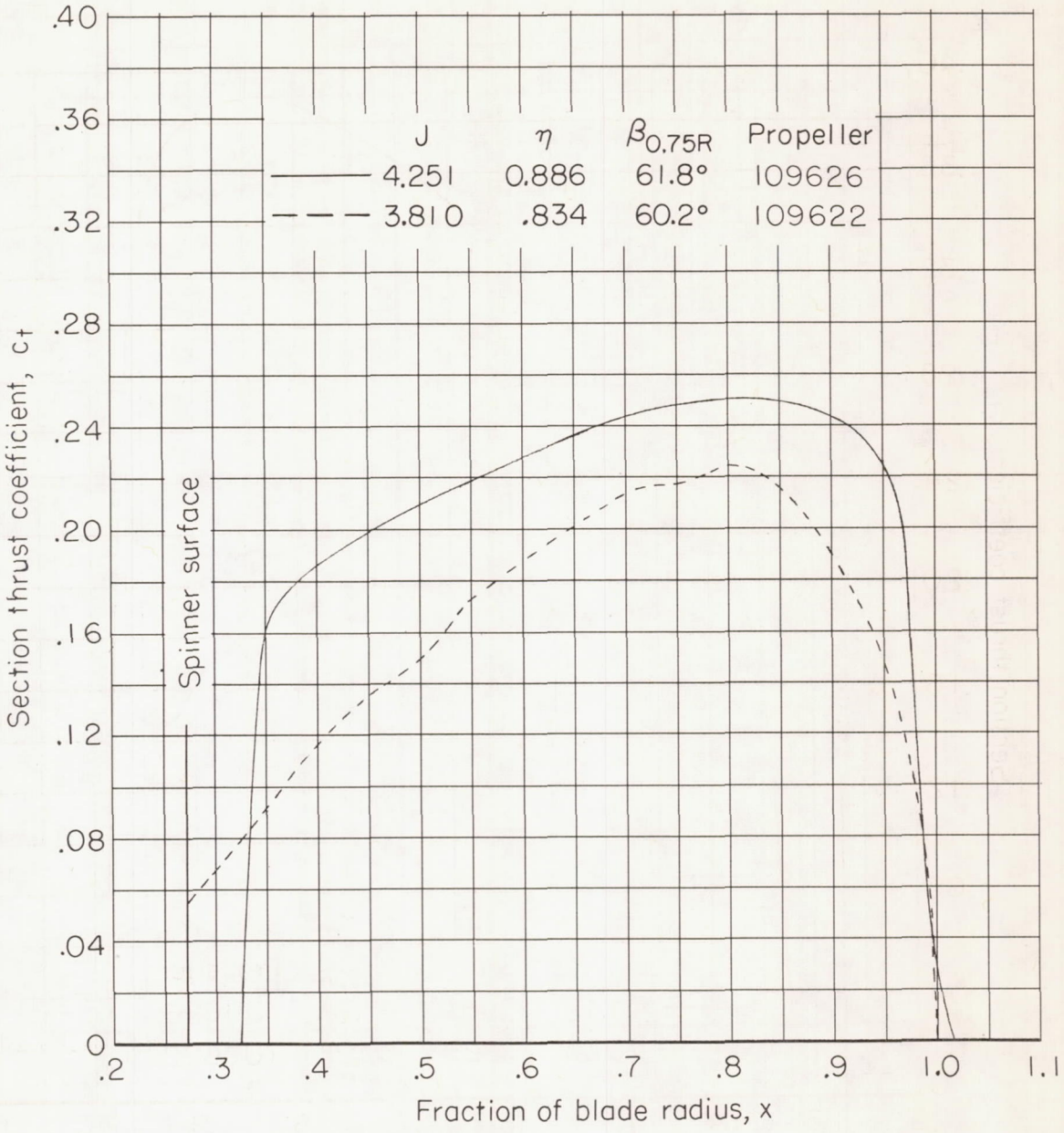
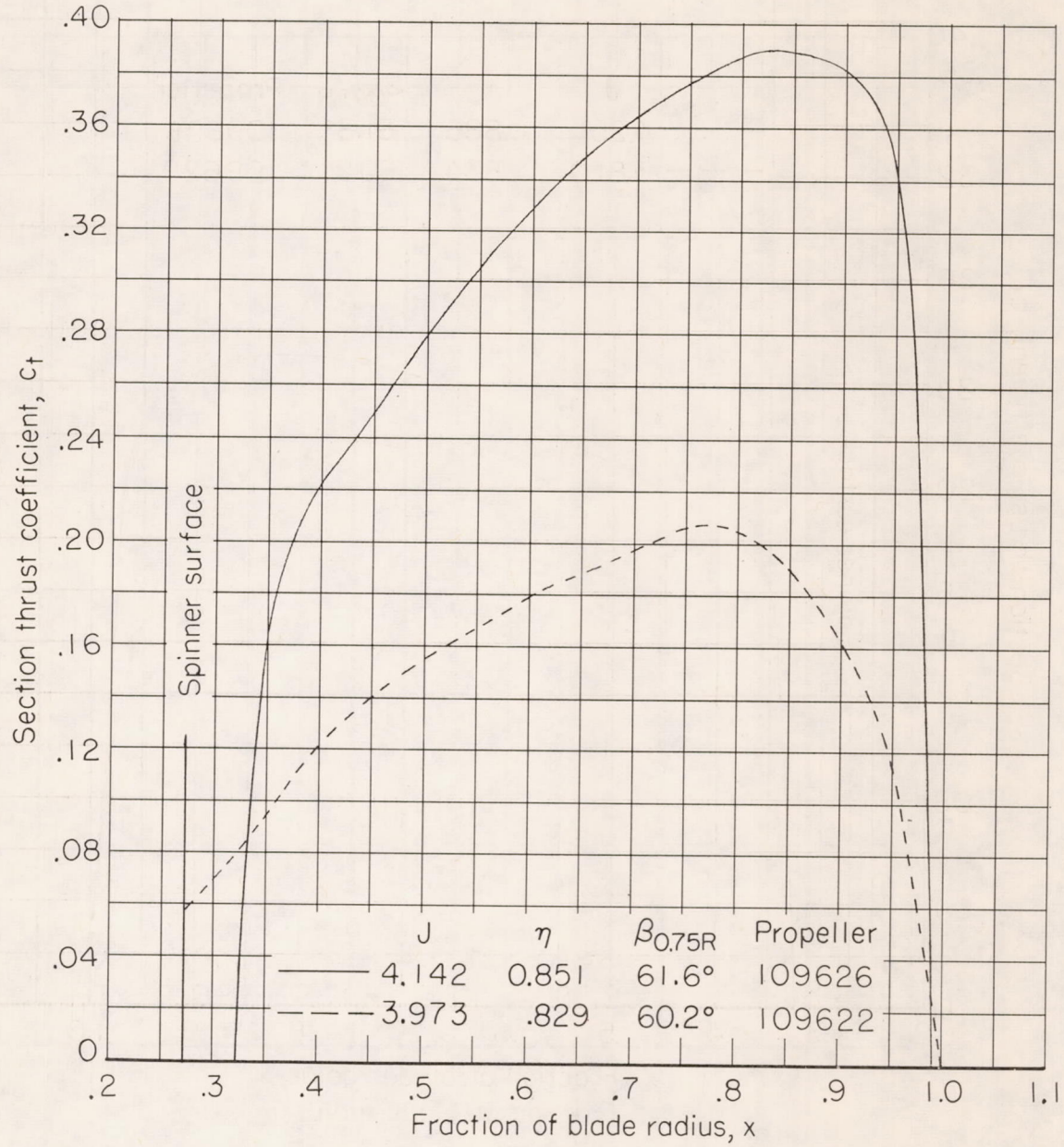


Figure 13.- Pitch distribution comparison of the 109626 and 109622 propellers with 1.4° pitch differential at the 0.75 radial station.



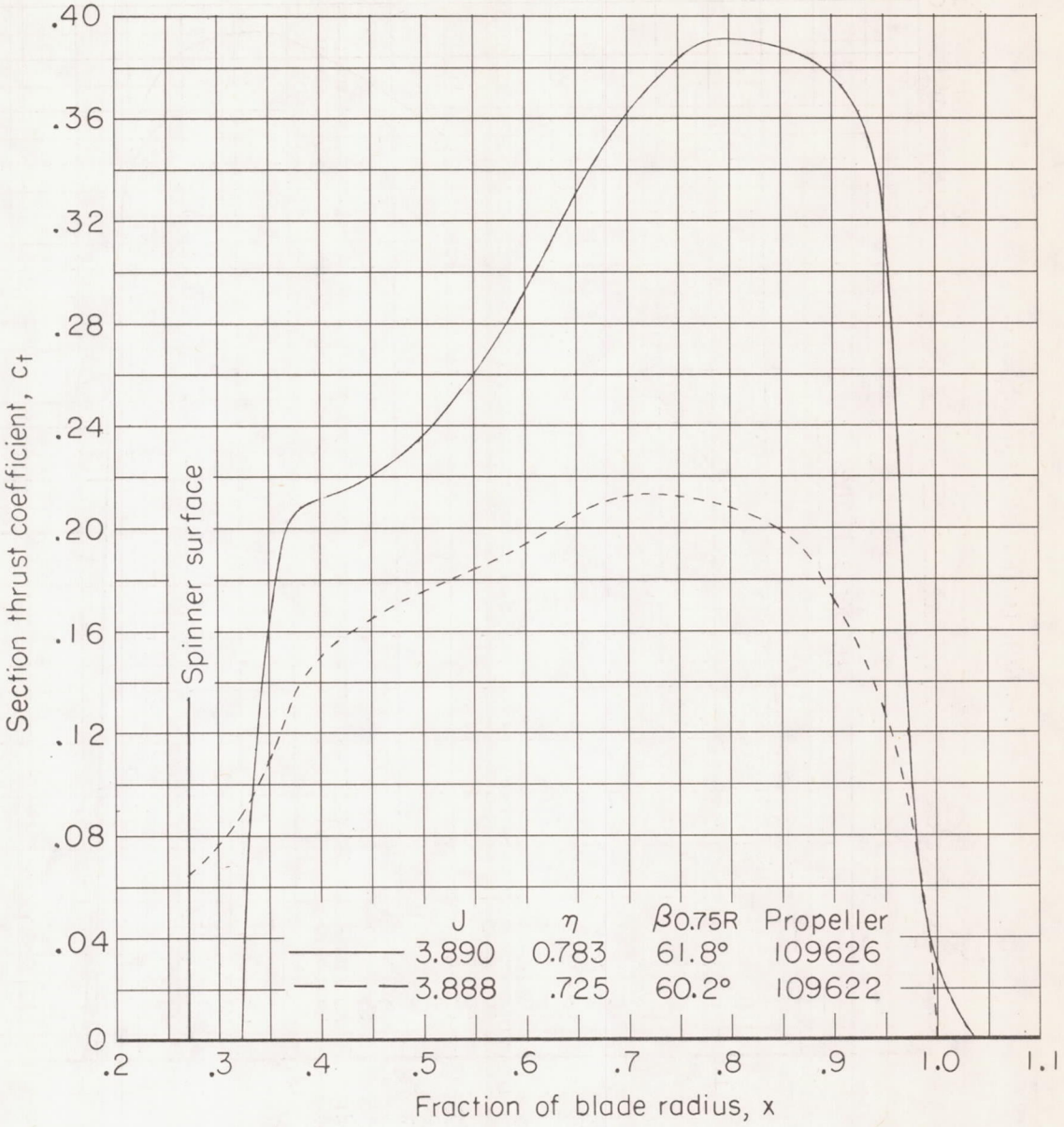
(a) M = 0.60.

Figure 14.- Thrust loading comparison of 109622 and 109626 propellers at advance ratios for maximum efficiency.



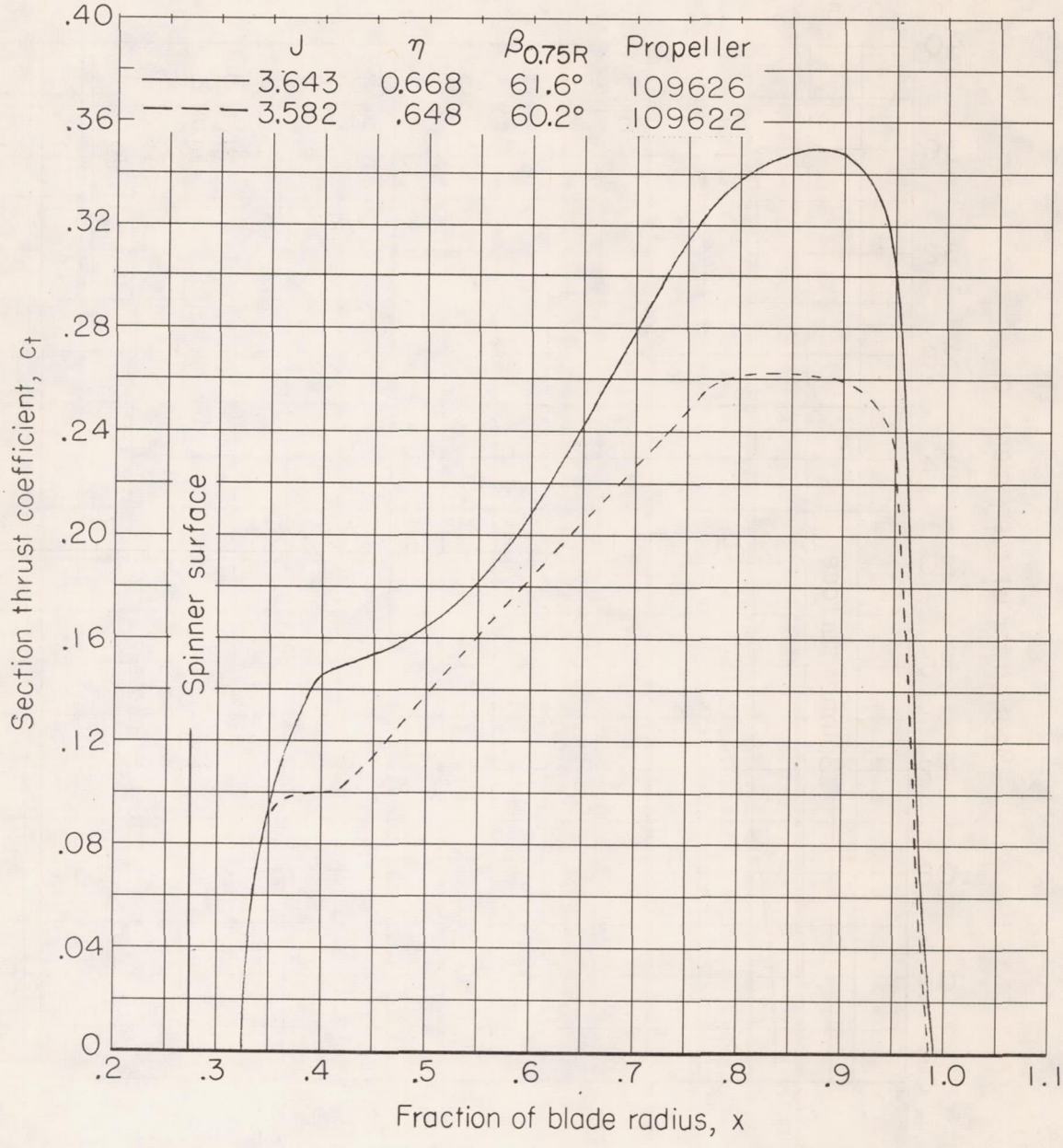
(b) M = 0.80.

Figure 14.- Continued.



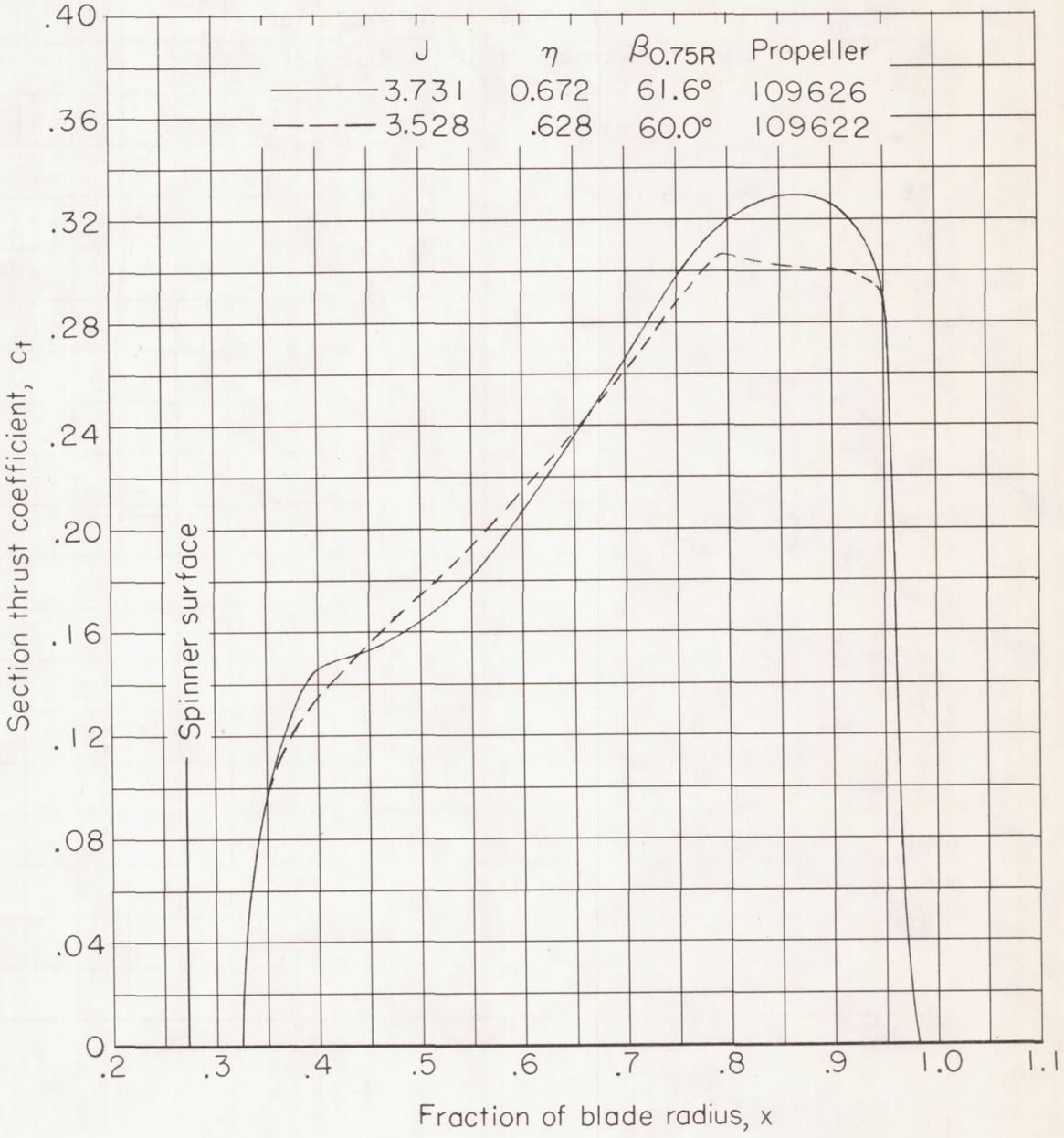
(c) M = 0.89.

Figure 14.- Continued.



(d) M = 1.00.

Figure 14.- Continued.



(e) M = 1.03.

Figure 14.- Concluded.